Isotopic evidence for a link between Lyra Basin and Ontong Java Plateau

Maria Luisa G. Tejada[1,2]†, Kenji Shimizu[1], Katsuhiko Suzuki[1], Takeshi Hanyu[1], Takashi Sano[3], Masao Nakanishi[4], Sun'ichi Nakai[5], Akira Ishikawa[6], Qing Chang[1], Takashi Miyazaki[1], Yuka Hirahara[1], Toshiro Takahashi[1], and Ryoko Senda[1]

[1]*Japan Agency for Marine-Earth Science and Technology, Yokosuka, 237-0061 Japan*

[2]*National Institute of Geological Sciences, University of the Philippines, Diliman, Quezon City, 1101 Philippines*

[3]*Department of Geology and Paleontology, National Museum of Nature and Science, Tsukuba, 305-0005 Japan*

[4]*Graduate School of Science, Chiba University, Chiba, 263-8522 Japan*

[5]*Earthquake Research Institute, University of Tokyo, Tokyo, 153-8902 Japan*

[6]*Department of Earth Science and Astronomy, University of Tokyo, Tokyo, 153-8902 Japan*

†Corresponding author (e-mail: mtejada@jamstec.go.jp)

Submitted to the GSA Special Volume on Oceanic LIPs

ABSTRACT

The few geological and geophysical studies of the Lyra Basin at the western margin of the Ontong Java Plateau (OJP) revealed that it is underlain by thicker than normal oceanic crust. The unusually thick oceanic crust is attributed to the emplacement of massive lava flows from the OJP. Dredging was conducted to sample the inferred OJP crust on the Lyra Basin but instead recovered younger extrusives that may have covered the older plateau lavas in the area. The Lyra Basin extrusives are alkalic basalts with $(^{87}Sr/^{86}Sr)_t$ = 0.704513-0.705105, $(^{143}Nd/^{144}Nd)_t$ = 0.512709-0.512749 ($\varepsilon_{Nd}(t)$ = +3.0 to +3.8), and $(^{206}Pb/^{204}Pb)_t$ = 18.488-18.722, $(^{207}Pb/^{204}Pb)_t$ = 15.558-15.577, and $(^{208}Pb/^{204}Pb)_t$ = 38.467-38.680 that are distinct from those of the OJP tholeiites. They have age-corrected $(^{187}Os/^{188}Os)t$ = 0.1263-0.1838 that overlap with the range of values determined for the Kroenke- and Kwaimbaita-type OJP basalts but their $(^{176}Hf/^{177}Hf)t$ = 0.28295-0.28299 and $\varepsilon_{Hf}(t)$ = +7.9 to +9.3 values are lower. These isotopic compositions do not match those of any Polynesian ocean island volcanics well either. Instead, the Lyra Basin basalts have geochemical affinity and isotopic compositions that overlap with those of some alkalic suite and alnöites in the island of Malaita, Solomon Islands. Although not directly related to the main plateau volcanism at 120 Ma, the geochemical data and modeling suggest that the origin of the Lyra Basin alkalic rocks may be genetically linked to the mantle preserved in the OJP's thick lithospheric root, with magmatic contribution from the Rarotongan hotspot.

Components: 242 words abstract, 5629 words main text, 8 figures, 4 tables

Key words: Lyra Basin, Ontong Java Plateau, Pb-Nd-Sr-Os-Hf isotopes, late-stage volcanism, Malaita alkalic rocks, Malaitan alnöites, OJP lithospheric mantle root

1. INTRODUCTION

The Ontong Java Plateau (OJP), Manihiki Plateau (MP), and Hikurangi Plateau (HP) have been suggested to form one igneous complex despite their widely separated locations (Fig. 1a; Taylor, 2006; Hoernle et al., 2010; Timm et al., 2011; Chandler et al., 2012), based on similar ranges of age and isotopic composition. Similarly, areas around the OJP are also suggested to be part of the "Greater Ontong Java Plateau" (Ingle and Coffin, 2004; Taylor, 2006; Timm et al., 2011). For example, unusually thick, old oceanic crust to the north and east of the OJP in Mariana Basin and Nauru Basin, respectively, are attributed to the emplacement of a large volume of thick lava flows and sills from the plateau based on geochemical and geophysical data (Saunders, 1986; Castillo et al., 1991; 1994; Mochizuki et al., 2005). However, the area to the west of the plateau, in the Lyra Basin (Figs. 1 and 2), is unexplored or barely studied.

Limited geological and geophysical evidence also indicates a possible relationship between the OJP and Lyra Basin. Kroenke (1972) previously suggested that the Lyra Basin is a foundered section of the OJP based on the basin's horst and graben structures. More recent two-dimensional modeling across one OJP-Lyra transect also indicates the presence of thicker than normal oceanic crust in the Lyra Basin, which could suggest that it forms a contiguous part of the OJP, although velocity data are still needed to better resolve this hypothesis (Gladczenko et al., 1997). Rayleigh wave tomography of the OJP likewise suggests that OJP lavas must have spilled over its western margins based on the thicker than normal crustal thickness of 23 km under the Lyra Basin (Richardson et al., 2000). The present study

82 is the first geochemical investigation of the possible extension of the OJP's
83 emplacement along its western margins through the isotopic analysis of basement
84 rocks recovered from the Lyra Basin. We obtained the first set of Pb-Nd-Sr and Os-Hf
85 isotope data for the Lyra Basin lavas to better understand their origin and possible
86 relationship with the OJP.
87
88 **2. GEOLOGICAL BACKGROUND**
89
90 A geophysical survey was conducted by R/V Kairei of Japan Agency for
91 Marine-Earth Science and Technology (JAMSTEC) in December 2006 to probe the
92 tectonic history and origin of the Lyra Basin. The geophysical survey revealed that the
93 Lyra Basin is traversed by the Lyra Trough, a broad and deep graben, with 500 meter-
94 high lineated ridges near the middle and bounded by a fault scarp in its eastern margin
95 (Fig. 2, Nakanishi et al., 2007). Several seamounts were also identified in the eastern
96 rim of the basin. Basement rocks were recovered by dredging at two locations, one at
97 the lineated ridge near the middle part of the basin and one at the base of the slope of
98 one of the seamounts in the eastern margin (D1 and D2, respectively; Fig. 2).
99 A complementary petrological, geochronological, and geochemical study of
100 rocks dredged from both sites (Shimizu et al., this volume) reveals that they are
101 olivine-titanaugite phyric alkaline basalts and picrites that are products of very small
102 degree melting. An age of 65±1.3 Ma was obtained for the groundmass of an
103 unaltered sample from D2. This age suggests that the samples were produced by
104 seamount volcanism in the eastern margin of the Lyra Basin and possibly overlying
105 older Early Cretaceous OJP lavas inferred to comprise the basement of the basin. The
106 few single-channel seismic profiles available to date also suggest that the entire Lyra

Basin may be covered by post-OJP emplacement extrusives (Gladczenko et al., 1997). The younger age of the Lyra Basin basalts also reinforces the evidence for the ~ 60 Ma volcanic activity on the plateau as indicated by previous work in San Cristobal (Birkhold-Van Dyke et al., 1996). The relationship of these 65 Ma extrusives and the other younger, 44 Ma and 34 Ma, volcanic episodes with the main OJP volcanism (e.g., Tejada et al., 1996; Simonetti and Neal, 2010) is yet unclear.

3. SAMPLES AND METHODS

About fifty kg of basalts and picritic rocks were acquired by dredging from sites D1 and D2 (Fig. 2), with most of the samples coated with an Fe-Mn crust. Detailed descriptions of the samples are reported by Shimizu et al. (this volume). The rocks range from unaltered to highly altered, with fragment sizes varying from several millimeters to tens of centimeters. The unaltered samples are clinopyroxene-olivine phyric alkalic basalts (Fig. 3a) with 41-46 wt% SiO_2, 5-22 wt% MgO, 2-4 wt% TiO_2, and 1-5 wt% Na_2O+K_2O (Shimizu et al., this volume), which are compositionally different from OJP tholeiites with ~50 wt% SiO_2, ~8 wt% MgO, ~1 wt% TiO_2, and ~2 wt% Na_2O+K_2O (Mahoney et al., 1993; Tejada et al., 1996; 2002; Neal et al., 1997; Fitton and Godard, 2004). The alkalic nature of these rocks is also shown by the much higher concentrations of Zr and Nb (and other incompatible elements, Fig. 3b), falling within the range of data for ocean island basalts (OIB). There are no distinct petrological and geochemical differences between samples from the two dredge sites. Their compositional characteristics are also different from those of the OJP tholeiites but are similar to the younger, transitional to alkalic basalts, found associated with plateau lavas in Santa Isabel and Malaita in the Solomon Islands (Tejada et al., 1996).

Isotopic data for Pb, Nd, Sr, Hf, and Os for Lyra Basin alkalic basalts were acquired using the analytical facilities at JAMSTEC (Tables 1 and 2). Samples were first trimmed of Fe-Mn crusts and altered margins and reduced to smaller pieces by sawing with water lubricant. Then, they were cleaned of saltwater residues by desalination in a warm bath with continuously flowing distilled deionized water (DDW) for several days. Samples were rinsed in ultrapure milli-Q water several times and after the wash solution stays clear upon addition of $AgNO_3$ solution, they were dried in an oven at 110^{o}C for two days, and crushed while wrapped in paper using an iron mortar and pestle. The sample chips were cleaned again by sequentially sonicating in DDW, until loose, fine particles were removed, and by rinsing in milli-Q water and acetone. Further removal of chips with alteration stains and remaining saw marks was conducted under a magnifier after drying the samples in an oven at 110^{o}C for at least 24 hours. The picked chips, visibly free of alteration, were then powdered in an alumina mill and splits of powders were processed separately for Nd-Sr, Pb, Os, and Hf isotope composition determinations, respectively (Tables 1 and 2).

All sample powders were leached with 2.5M HCl at 80^{o}C for 8 hours prior to Sr, Nd, and Pb isotope analyses. Clinopyroxene separates were also leached with 1M HCl at room temperature for a day and then rinsed in ultrapure water and dried before dissolution. Different splits of the same leached whole rock powders were digested for Sr-Nd and for Pb isotopic analyses, respectively. Elemental abundances for Rb, Sr, Sm, Nd, Th, U, and Pb (Table 3) were measured by inductively-coupled-plasma spectrometry (ICPMS) on splits (~5%) of solutions used for Sr and Nd isotope analyses using an Agilent 7500ce (Chang et al., 2002).

For Sr and Nd isotope ratio determination, 120 mg of leached powders were decomposed with a 1:3 mixture of 12M $HClO_4$ and 20M HF followed by digestion in

157 1:3 mixture of 12M $HClO_4$ and 6M HCl, and then in 6M HCl, respectively, following
158 the procedures of Takahashi et al. (2009) and Hirahara et al., (2009; 2012). After
159 dissolution, solutions were split for parent-daughter concentration measurement and
160 Sr-Nd isotope analysis. Sr and Nd were purified from about 17% split of solutions by
161 established two-step cation exchange column procedures and were measured by
162 thermal ionization mass spectrometer (TIMS, TRITON). The procedural blanks were
163 typically <30 and <5 pg for Sr and Nd, respectively. Results for standards ran during
164 the measurement of Lyra Basin samples are $^{87}Sr/^{86}Sr = 0.710262 \pm 4$ for SRM 987 (n
165 = 7, 2SD) and $^{143}Nd/^{144}Nd = 0.512101 \pm 12$ for JNd-1 (n = 4, 2SD), equivalent to
166 $^{143}Nd/^{144}Nd = 0.511844$ for La Jolla Nd standard (Tanaka et al., 2000; Miyazaki et al.,
167 2012).

168 For Pb isotope analysis, about 100 mg of leached powders were decomposed
169 with a 1:4 mixture of 15M HNO_3 and 20M HF followed by digestion in 8M HBr.
170 Samples were then dissolved in 0.5M HBr prior to Pb separation by an anion
171 exchange column procedure using Bio-Rad AG-1X8 resin (200-400 mesh). After
172 chemical separation, the Pb isotopic compositions were measured through the double-
173 spike method described by Miyazaki et al. (2009). The chemically separated Pb
174 aliquot of each sample was split into two, one of which was doped with a spike
175 enriched in two isotopes ^{207}Pb and ^{204}Pb. Both were measured by TIMS for Pb isotope
176 ratios with a common denominator (i.e., either $^{206, 207, 208}Pb/^{204}Pb$, or $^{204,207,208}Pb/^{206}Pb$,
177 or $^{204, 206, 208}Pb/^{207}Pb$, or $^{204,206, 207}Pb/^{208}Pb$) and the isotopic composition of the sample
178 was derived using values for unspiked and spiked aliquots. The isotopic compositions
179 of the ^{207}Pb-^{204}Pb double spike, normalized to NIST SRM 982 standard $^{208}Pb/^{206}Pb =$
180 1.00016, are $^{206}Pb/^{204}Pb = 0.10203$, $^{207}Pb/^{204}Pb = 3.8717$, and $^{208}Pb/^{204}Pb = 0.18865$.
181 Total procedure blank is <5 pg and the measured values for NIST 981 standard are

182 $^{206}Pb/^{204}Pb$ = 16.939 ± 4 (n=4, 2 SD), $^{207}Pb/^{204}Pb$ = 15.497 ± 4 (n=4, 2 SD) and
183 $^{208}Pb/^{204}Pb$ = 36.721 ± 9 (n=4, 2 SD).

184 For Os isotope ratios and Re and Os concentration measurements, 1-2 g of
185 unleached powders were weighed, combined with Re and Os spikes and sealed in
186 Carius tubes with 2.5 ml and 7.5 ml of concentrated 9M HCl and 16M HNO_3,
187 respectively. Digestion of samples was conducted at 220-230^{o}C for 38 hours, after
188 which Os was separated by solvent extraction followed by microdistillation, while Re
189 was purified by an anion exchange column separation method (Cohen and Waters,
190 1996; Roy-Barman and Allegre, 1995; Pearson and Woodland, 2000). Re and Os
191 were measured as oxides by TIMS in negative ion mode at JAMSTEC's Re-Os
192 isotope laboratory. Analytical procedures followed those described by Suzuki et al.
193 (2004) and Tejada et al. (2013). Total procedure blanks are 2.7 ppt for Os and 4.2 ppt
194 for Re. Blank contributions are negligible: 0.4% (D1-06) to 8.6% (D2-02) for Os and
195 2.1% (D1-06) to 7.4% (D2-02) for Re. Data for samples with >10% blank
196 contribution due to very low Os contents are not reported in Table 2.

197 Analytical procedures for determining Hf isotope composition followed those
198 described by Hanyu et al. (2005). Briefly, 100 mg splits of the same powders used for
199 Os isotope determination were weighed and mildly leached in 2N HCl for 10 minutes
200 in ultrasonic cleaner. The leached powders were then rinsed three times with milli Q
201 water and digested at 160^{o}C for at least 24 hours using a 1:2 mixture of 12M $HClO_4$
202 and 25M HF. After evaporation, the digested samples were then dried and dissolved
203 in 3M HCl and evaporated again. Dried samples were then re-dissolved in 5 ml of 3M
204 HCl and split for abundance measurement (20%) and isotope ratio determination
205 (80%). Splits for Lu and Hf abundance analysis were dried and dissolved in 5 ml
206 0.4M HNO_3: 0.5M HF solution mixed with indium (In) internal standard and

measured using Quadrupole ICPMS (Agilent 7500ce) at JAMSTEC following the methods of Chang et al. (2002). For isotope ratio determination, Hf was separated and purified in a two-step column extraction procedure and stored in 3 ml of 0.4M HNO_3: 0.1M HF just before analysis on the ISOPROBE multicollector ICPMS at the Earthquake Research Institute, University of Tokyo. The $^{176}Hf/^{177}Hf$ value obtained for rock standard JB-1b is 0.282973 ± 0.000010, corresponding to $\varepsilon_{Hf} = +7.1 \pm 3$. This value is similar to previously published range of data for this rock standard (mean $^{176}Hf/^{177}Hf = 0.282990$, SD = 16, n=3; Hanyu et al., 2005).

3. RESULTS

3.1. Pb-Nd-Sr isotopes

Lyra Basin basalts have age-corrected isotopic compositions of $(^{87}Sr/^{86}Sr)_t$ = 0.704513-0.705105, $(^{143}Nd/^{144}Nd)_t$ = 0.51271-0.51275 [$\varepsilon_{Nd}(t)$ = +3.0 to +3.8], $(^{206}Pb/^{204}Pb)_t$ = 18.488-18.722, $(^{207}Pb/^{204}Pb)_t$ = 15.558-15.577, and $(^{208}Pb/^{204}Pb)_t$ = 38.467-38.680 (Table 1, Figs. 4-5). These ratios are distinct from those of the OJP tholeiites but consistently plot close to those of the North Malaitan alkalic rocks, except for their Sr isotopic composition. Apart from their lower $(^{207}Pb/^{204}Pb)_t$, their isotopic compositions overlap with those of Malaitan alnöites (Figs. 4-5), with age-corrected (t = 34 Ma) $(^{87}Sr/^{86}Sr)_t$ = 0.704156-0.704642, $(^{143}Nd/^{144}Nd)_t$ = 0.51270-0.51279 ($\varepsilon_{Nd}(t)$ = +2.0 to +3.8), $(^{206}Pb/^{204}Pb)_t$ = 18.673-18.687, $(^{207}Pb/^{204}Pb)_t$ = 15.598-15.600 and $(^{208}Pb/^{204}Pb)_t$ = 38.496-38.515 (Bielski-Zyzkind et al., 1984; Neal and Davidson, 1989; Ishikawa et al., 2007). In summary, although the isotopic compositions of the Lyra Basin basalts are distinct, they plot closely with the data for

232 OJP and Malaitan alkalic rocks and overlap with alnöite data field in most isotope
233 diagrams, suggesting some connection in their origins.

234 The clinopyroxene separates have similar Sr and Nd isotopic composition with
235 the lavas, as expected (Table 1; Fig. 4a). Age-corrected values are $(^{87}Sr/^{86}Sr)_t$ =
236 0.704863-0.705100 and $(^{143}Nd/^{144}Nd)_t$ = 0.51270-0.51272 [$\varepsilon_{Nd}(t)$ = +2.8 to +3.3],
237 which are well within the range of values obtained from the whole rocks.
238 Interestingly, the isotopic composition of the Lyra Basin basalts and clinopyroxene
239 separates are also within the range of some pyroxenite xenoliths brought to the
240 surface by the Malaitan alnöite intrusions (Ishikawa et al., 2007). These pyroxenite
241 xenoliths appear to have affinities for both the Kroenke-Kwaimbaita-type OJP
242 tholeiites and the Lyra Basin alkalic basalts, suggesting a possible relationship with
243 both.

244 Compared to South Pacific ocean island basalts (OIBs) that are presumed to be
245 products of hotspot magmatism (Devey et al., 2003; Bonneville et al., 2006; Castillo
246 et al., 2007; Koppers et al., 2008; Jackson et al., 2010), the isotopic compositions of
247 the Lyra Basin alkalics overlap with data for Samoan shield basalts, particularly from
248 Ta'u and Ofu islands (Fig. 4) but their Pb isotope compositions are lower and only
249 slightly overlap with the estimated age-corrected data fields for the latter (Fig. 5).
250 Their Pb isotopic composition overlaps with those of Rarotonga in both $^{207}Pb/^{204}Pb$
251 and $^{208}Pb/^{204}Pb$ diagrams. However, their Sr and Nd isotopic compositions are quite
252 distinct from those of the Rarotongan lavas. Interestingly, no single group of present-
253 day (Vidal et al., 1984; Wright and White, 1987; Palacz and Saunders, 1986;
254 Nakamura and Tatsumoto, 1988; Woodhead and Devey, 1993; Schiano et al., 2001;
255 Lassiter et al., 2003; Hart et al., 2004; Bonneville et al., 2006; Castillo et al., 2007;
256 Jackson et al., 2007; 2010; Koppers et al., 2008; Hanyu et al., 2011) or equivalent

257 Cretaceous Polynesian hotspot OIBs (Koppers et al., 2003; Konter et al., 2008;
258 Shimoda et al., 2011) closely match the Sr-Nd-Pb isotopic compositions of the Lyra
259 Basin basalts.
260
261 **3.2. Os-Hf isotopes**
262
263 The Lyra Basin basalts have age-corrected $(^{187}Os/^{188}Os)_t$ = 0.1263-0.1838 and
264 $(^{176}Hf/^{177}Hf)_t$ = 0.28295-0.28298 [$\varepsilon_{Hf}(t)$ = +7.9 to +9.3] (Table 2). Their Os isotopic
265 composition overlaps with those of the Kroenke- and Kwaimbaita-type OJP tholeiites
266 (0.1322±0.0029 and 0.1395±0.0020, respectively; Tejada et al., 2013). Like the
267 Kwaimbaita-type OJP basalts, the higher $(^{187}Os/^{188}Os)_t$ values may be attributed to
268 assimilation during ascent through altered MORB crust, inferred to be present beneath
269 Malaita (Ishikawa et al., 2004; 2005). This observation is also consistent with their
270 elevated $(^{87}Sr/^{86}Sr)_t$ ratios (Fig. 4; Neal and Davidson, 1989).
271 The $\varepsilon_{Hf}(t)$ values of the Lyra Basin basalts are lower than the OJP tholeiites.
272 The data fall along the mantle array in $\varepsilon_{Nd}(t)$ vs. $\varepsilon_{Hf}(t)$ plot, away from the trend of the
273 plateau data (Fig. 6). However, they appear to plot toward or closer to the Os and Hf
274 isotopic composition fields for Malaitan alnöite and pyroxenites. Interestingly, the
275 Lyra Basin data plot within the data field of Samoan shield lavas in Hf-Nd-Os isotope
276 plots, although their Pb isotope compositions just slightly overlap with the lower
277 range of the latter (Fig. 5).
278 Lyra Basin basalts have generally lower Re (58-326 ppt) than, but similar
279 range of Os (31-91 ppt, except for the high MgO sample D1-06 with Os up to 741
280 ppt) to those of Malaitan Kwaimbaita-type OJP tholeiites (Re = 1306-1345 ppt; Os =
281 11-51; Tejada et al., 2013). Their Re concentrations are higher in range, but Os values

282 are much lower, than those of the alnoites (Re = 27.5-36.5 ppt; Os = 478-811 ppt;
283 Ishikawa et al., 2011). Compared with Pacific OIBs, Lyra Basin alkalic basalts have
284 similar ranges for Re and $^{187}Os/^{188}Os$ to, but their Os is slightly lower than, those of
285 Samoan shield lavas from Ta'u (Re = 44-423 ppt; Os = 115-325, except for high MgO
286 sample with Os = 5630 ppt; $^{187}Os/^{188}Os$ = 0.1283-0.1310; Jackson and Shirey, 2011)
287 and Ofu islands (Re = 38-190 ppt; Os = 67-240; $^{187}Os/^{188}Os$ = 0.1287-0.1294; Jackson
288 and Shirey, 2011). Rarotongan basalts have a slightly higher range of Re but similar
289 Os contents and isotope composition (Re = 230-606, ppt Os = 3-121 ppt, $^{187}Os/^{188}Os$
290 = 0.1243-0.1415; Schiano et al., 2001; Hanyu et al., 2011) to Lyra Basin basalts.
291 However, Rarotongan lavas have lower $\varepsilon_{Nd}(t)$ and $\varepsilon_{Hf}(t)$ values (e.g., 0.2 to +1.6 and
292 +4.0 to +5.8, respectively; Schiano et al., 2001; Hanyu et al., 2011) than the basin
293 lavas (Figs. 4 and 6).
294
295 **4. DISCUSSION**
296
297 What is the meaning of the close ranges of isotopic composition among Lyra
298 Basin basalts, North Malaitan alkalic suite and Malaitan alnöites and pyroxenites?
299 Can Lyra Basin basalts represent the proto-alnöite alkali magma postulated to have
300 been the melt from which the megacrystic xenoliths crystallized and fractionated
301 further to become the alnöite magma (Neal and Davidson, 1989) 10-30 Ma later? Or
302 are they an expression of a recycled, more fusible, component in a hybrid or
303 composite OJP plume mantle source (Ishikawa et al., 2007; 2011)? Can the Lyra
304 Basin alkalics be derived from the same OJP mantle source? Since the ($^{87}Sr/^{86}Sr$)
305 values are easily changed by seafloor alteration processes and although the leaching

306 procedure should help recover the magmatic values, we do not emphasize the Sr
307 isotope data in the following discussion.
308
309 **4.1. Relationship with younger alkalic volcanism on the OJP**
310
311 The younger age (65 Ma) of the Lyra Basin basalts relative to that of the main
312 OJP eruption (122 Ma) indicates that the origin of the former is more related to that of
313 the young alkalic suites (44 Ma) in Malaita. Previous work (Tejada et al., 1996)
314 suggested that the younger alkalic suites in Malaita, especially the Younger Series and
315 North Malaita (or Maramasike Formation; Petterson et al., 1997), may have been a
316 consequence of OJP's passage over the Samoan and Rarotongan hotspots at around
317 the same time. This is supported by plate reconstructions showing that the OJP passed
318 directly over these hotspots between ~60 and ~30 Ma (Fig. 7, Natland, 1985; Yan and
319 Kroenke, 1993; Chandler et al., 2012). Furthermore, the HIMU-like characteristics of
320 the 92 Ma Sigana Alkalic suite in Santa Isabel (Tejada et al., 1996) may have been
321 also an indication of the influence of the Cook-Austral hotspot, which has been active
322 since around 100 Ma (Koppers et al., 2003; Konter et al., 2008) and as far back as
323 ~120 Ma (Shimoda et al., 2011).
324 The 65 Ma age of the Lyra Basin basalts does not, however, fit the Samoan
325 hotspot connection. The oldest recovered trace of the Samoan signature in the present
326 South Pacific Polynesian lavas so far is the 23 Ma Alexa bank lavas (data field
327 marked S in Figs. 4-5; Hart et al., 2004), and the Lyra Basin alkalics have isotopic
328 compositions more akin to the younger expression of this hotspot from the shield
329 volcanics of Ta'u and Ofu islands (Jackson et al., 2007; 2010), also known as Manua
330 island (Wright and White, 1987). Instead, Lyra Basin basalts are more likely

connected to the Rarotongan hotspot, which has been in existence since ~110 Ma, based on backtracked position of the Magellan Seamount trail and the isotopic similarity between the trail volcanics and present-day lavas (Koppers et al., 2003; Konter et al., 2008). Figure 7 shows that the OJP passed over the Rarotongan hotspot also between ~80 to ~47 Ma, which encompassed the eruption of the Lyra Basin basalts. Combined with the existence of the Sigana Alkalic Suite in Santa Isabel, it can be envisioned that Polynesian hotspots left their imprint on the periodically erupted alkalic basalts from ~90 Ma, ~65 Ma, ~44 Ma, and ~34 Ma on the OJP. Any one or a combination of these hotspots along the OJP's path may have been both a source of heat and materials for the younger volcanism on the OJP.

4.2. Genetic link between Malaitan alnöite and Lyra Basin basalts?

The overlapping isotopic compositions of Lyra Basin alkalic rocks with those of Malaitan alnöites and some pyroxenite xenoliths, except for Hf isotopes, imply they too may have a petrogenetic connection. Neal and Davidson (1989) postulated the existence of an alkalic, proto-alnöite, magma predicted to have isotopic compositions close to those of augite megacrysts (incorporated into the alnöite magma) that have the least radiogenic isotopic values. Ion microprobe U-Pb dating of zircons separated from alnöite gave a range of ages from 35-49 Ma, interpreted to be an indication that they crystallized for a prolonged period of time from proto-alnöite magma (Kitajima et al., 2008). Another more recent work (Simonetti and Neal, 2010) also inferred that such proto-alnöite magma may have been crystallizing for a protracted period of time based on the wide range of ages, ~55 to ~35 Ma, derived from magmatic zircons associated with alnöites in northern Malaita. These zircons are

356 believed to have crystallized from alnöite magmas based on their identical $^{176}Hf/^{177}Hf$
357 (average = 0.282933; Simonetti and Neal, 2010). Although the Lyra Basin basalts
358 could represent this putative proto-alnöite magma, the augite megacrysts appear to
359 have more affinity with the Younger Series alkalic suite in terms of their $\varepsilon_{Nd}(t)$ values,
360 +0.8 to 1.9 for the augites (Neal and Davidson, 1989) vs. -0.5 to +1.0 for the Younger
361 Series basalts (Tejada et al., 1996). These results suggest that the proto-alnöite magma
362 may have isotopic compositions similar to those of the Younger Series alkalic suite
363 originally. To produce the isotopic composition of the Lyra Basin basalts and the
364 alnöites from the Younger Series, this latter component must have interacted with the
365 OJP lithospheric mantle source. Note that the composition of clinopyroxene
366 phenocrysts, which have crystallized earlier from the Lyra Basin magmas, also trend
367 toward lower $\varepsilon_{Nd}(t)$ values than the whole rocks (Table 1). Thus, the locations of Lyra
368 Basin and alnoite data between the fields for Kroenke-Kwaimbaita-type OJP and
369 Younger Series alkalic suite in the Nd-Pb-Hf isotope plots may be indicating a
370 petrogenetic relationship.

371 An analogous idea was put forward by Ishikawa et al. (2004), based on their
372 study of different types of xenoliths brought about by alnöite intrusions in Malaita.
373 They inferred the presence of alkalic magma representing melts from a more fusible,
374 recycled component encapsulated within unmelted peridotite in a hybrid OJP plume
375 mantle source that was amalgamated with the overlying plateau crust since around
376 120 Ma. The pyroxenite xenoliths associated with the alnöite magma are also inferred
377 to have originated as a melting residue of basaltic material that gave rise to the alkalic
378 magma (Ishikawa et al., 2004; 2007). Such magma may have remained isolated and
379 may have partly reacted with the enclosing peridotite to form the orthopyroxenites
380 and garnet-pyroxenite xenoliths that were also carried to the surface by the alnöite

381 magma. The alnöites are inferred to have evolved from this alkalic magma that has
382 remained untapped until the ~34 Ma eruption of the alnöite. Given the similar to
383 overlapping isotopic composition of the Lyra Basin lavas with those of the alnöite
384 (Figs. 4-6), except for the slight difference in Hf, it can be inferred that such proto-
385 alnöite, alkalic magma could have been tapped by volcanism as early as 65 Ma,
386 covering the Lyra Basin to the west of the OJP. Furthermore, the wider range of
387 isotopic composition of the pyroxenites encompassing both those of OJP basalts and
388 alnöite in all isotope plots, indicating interaction with both sources, also supports this
389 interpretation.
390
391 **4.3. Role of "fossil" OJP lithospheric plume mantle**
392
393 Geophysical evidence suggests the existence of rheologically strong chemical
394 mantle root beneath the OJP (Richardson et al., 2000; Klosko et al., 2001). A possible
395 interpretation for this is that melt extraction and the resulting depleted OJP plume
396 mantle may have formed a lithospheric "keel" that became coupled with the plateau
397 crust. The identification of the layered lithosphere beneath OJP, consisting of an
398 overlying MORB lithosphere and underlying OJP plume lithosphere, based on the
399 study of mantle xenoliths brought to the surface by alnöite eruption in Malaita
400 (Ishikawa et al., 2004) lends petrological and geochemical support for this
401 interpretation. However, the thickness of this lithospheric "keel" cannot be accounted
402 for by a melt-depleted residue only, which would have left behind a much thinner,
403 ~80 km, layer (Klosko et al., 2001). Thus, it can be inferred that additional, relatively
404 fertile, OJP plume mantle containing melt pockets contributes to the seismically and
405 chemically anomalous nature of the OJP lithospheric keel. These melt pockets could

406 also be stagnated small fractions of magma left behind by the main upwelling event
407 that formed the plateau at ~122 Ma and preserved within the lithospheric root
408 (Ishikawa et al., 2004). They could be the source of both Lyra Basin basalts and
409 alnöites.

410 The isotopic compositions of the North Malaita Alkalic Suite in northernmost
411 Malaita plot relatively close to the data fields for OJP tholeiites (Figs. 4-5), leading
412 Tejada et al. (1996) to postulate that they could represent small amounts of melting of
413 aged or "fossil" OJP plume mantle that got incorporated into the base of the OJP
414 lithosphere. In the same way, the Lyra Basin data are close to the data fields of
415 Kroenke-Kwaimbaita-type OJP basalts in all isotope plots (Figs. 4-6), pointing toward
416 an origin analogous with that of the North Malaitan alkalic suite. The lower $\varepsilon_{Nd}(t)$ vs.
417 $\varepsilon_{Hf}(t)$ values, higher $^{206P}b/^{204}Pb$, $^{207}Pb/^{204}Pb$, and $^{208}Pb/^{204}Pb$ ratios of the Lyra Basin
418 basalts compared to those of Kroenke-Kwaimbaita-type tholeiites appear to be
419 consistent with radiogenic ingrowth trend in the OJP lithospheric mantle source with
420 time. However, the change from Kroenke-Kwaimbaita-type OJP mantle source
421 composition to that of average Lyra Basin isotopic signature ($\varepsilon_{Nd}(t)$ = +3.3; ε_{Hf} (t) =
422 +8.5; $^{206P}b/^{204}Pb$ = 18.584, and $^{208}Pb/^{204}Pb$ = 38.571) within a ~55 Ma period requires
423 $^{147}Sm/^{144}Nd$, $^{176}Lu/^{177}Lu$, $^{238}U/^{204}Pb$ and $^{232}Th/^{204}Pb$ values of <0.01, <0.001, ~26 and
424 ~100, respectively. These values are quite unrealistic given the observed parent-
425 daughter ratios in relatively fresh OJP and Lyra Basin basalts ($^{147}Sm/^{144}Nd$ = 0.18-
426 0.29 vs. 0.12-0.13, $^{176}Lu/^{177}Hf$ = 0.020-0.034 vs. 0.0031-0.0046, $^{238}U/^{204}Pb$ =14-18 vs.
427 14-21 and $^{232}Th/^{204}Pb$ = 56-75 vs. 75-81), respectively. Note that $^{147}Sm/^{144}Nd$ and
428 $^{176}Lu/^{177}Hf$ would be higher and $^{238}U/^{204}Pb$ and $^{232}Th/^{204}Pb$ lower in the OJP
429 lithospheric mantle source than in the basalts after melting. But if garnet was
430 exhausted during the main OJP melting event, which is likely, the increase in Lu/Hf

and Sm/Nd in the residue would be muted. It is also likely that, if the OJP lithospheric mantle was the source of the Lyra Basin magmas, its trace element contents must have been modified fairly recently or after the formation of the plateau basalts. Alternatively, the Lyra Basin alkalics, including those represented by the younger alkalic volcanism, could be the manifestation of small-scale heterogeneities intrinsic to the OJP plume itself (Tejada et al., 1996).

4.3.1. Contribution from Rarotongan hotspot

One mechanism capable of modifying the OJP lithospheric mantle is by interaction with melts or metasomatic fluids. As noted in section 4.1, the location of Lyra Basin data between the fields for Kroenke-Kwaimbaita-type OJP and Rarotonga in the isotopic space indicates the possibility that the source of the Lyra Basin basalts may have been a product of mixing OJP and Rarotonga sources. We now try to model this scenario using the Kroenke-type OJP composition and Rarotongan basalts as end members. We model the Lyra Basin composition as a product of mixing Rarotongan melts and OJP lithospheric mantle source (Table 4). The modeling results show that the Lyra Basin basalt composition can be explained by ~12-22% contribution of Rarotongan melts to the OJP lithospheric mantle (Fig. 8), although it is not clear on Pb-Os isotope plot (not shown). These results suggest that the OJP lithospheric mantle may have been fertilized extensively by melts from the Rarotongan hotspot prior to the generation and eruption of the Lyra Basin basalts from about ~80 Ma to ~45 Ma. Interestingly, the Rarotongan isotopic signature seems to have been retained in the composition of the ~44 Ma Younger Series alkalic lavas in Southern Malaita. Furthermore, the suggestion of Neal and Davidson (1989) of a proto-alnöite alkalic magma, whose composition is approximated by the least enriched augite megacryst

456 with Nd isotopic composition similar to the Younger Series alkalic basalts, is
457 consistent with this interpretation. Trace element modeling of the Lyra Basin data is
458 also in agreement with derivation by ~12% partial melting from the same near-
459 chondritic source inferred for the OJP basalts, mixed with very small degree melts of
460 Rarotongan source (see also Shimizu et al., this volume).

461 A potential problem with involving another hotspot source is the presence of
462 an attached very thick lithospheric root underneath the OJP. Given this thick
463 lithospheric root, magmas with pure Rarotongan signature are not to be expected,
464 unless tapped by very deep fractures or faults and escaped reaction with surrounding
465 country rock. It is more likely that melts from this source would have mixed with and
466 metasomatized the OJP lithospheric mantle before being erupted. Some of these melts
467 may have found their way around the lithospheric root, in the same way that
468 asthenospheric flow is deflected around it today (Klosko et al., 2001), and may have
469 been erupted under thinner lithosphere at the margins of the OJP. Thus, it is not
470 surprising that both the Malaitan alkalic suites and alnöites, as well as the Lyra Basin
471 basalts, occur along the southern and western margins of the plateau, respectively.
472 The only difference is that the Lyra Basin basalts might have been derived from the
473 mixed source formed by interaction of Rarotongan melts with the OJP lithospheric
474 mantle, whereas the Malaitan alkalic suite, particularly the Younger Series extrusives
475 may have originated from less modified Rarotongan mantle-derived magmas.
476 Furthermore, some of the excess thickness of the OJP lithospheric root (Klosko et al.,
477 2001) may in fact be attributed to the additional mechanical coupling of the melting
478 residue from Rarotongan (and Samoan) plume mantle, consistent with this model.
479 Whether such contributions could generate the observed mantle root thickness
480 remains to be seen.

481

482 ***4.3.2. Lyra Basin source component in the OJP plume lithospheric mantle***

483 A simpler way to explain the origin of the Lyra Basin basalts is by derivation
484 from melts of a minor, more fusible component in the OJP lithospheric mantle that
485 remained untapped until 65 Ma and ~34 Ma (as alnöite). In this scenario, the Lyra
486 Basin isotopic composition was not expressed in the 120 Ma eruption possibly
487 because it may have been swamped by the more dominant main OJP mantle source
488 signature. The decreasing Re contents and increasing Os abundances from the OJP
489 basalts to Lyra alkalics to alnöites indicate a progressively melt-depleted mantle
490 source. This suggests that the Lyra Basin and alnöite sources may have experienced
491 larger degrees of melting than the near-primitive mantle source inferred for the
492 Kroenke-Kwaimbaita-type OJP basalts. These pockets of mantle that experienced
493 higher degree of melting could have been incorporated or encapsulated within the
494 main OJP mantle source from the beginning and some may have remained untapped
495 until eruption at 65 Ma. If true, the combined alkalic volcanism at 90 Ma, 65 Ma, 44
496 Ma, and 35 Ma could represent the late-stage evolution in the OJP's hotspot
497 development after the plume head activity represented by the main plateau
498 emplacement.

499 The interpretation that the source of Lyra Basin basalts is intrinsic within the
500 OJP mantle itself still begs the question of a mechanism for the OJP lithospheric
501 mantle source to remain at or near-liquidus temperature for ~60 Ma after the main
502 plateau emplacement event. The lack of heat flow anomaly today, combined with
503 apparent rheological strength, suggests that it is unlikely that the lithospheric root
504 under the OJP is thermally maintained (Richardson et al., 2000; Klosko et al, 2001).
505 Reheating due to OJP's passage over the South Pacific Polynesian hotspot region may

506 have provided the mechanism for melting and magmatism responsible for the alkalic
507 volcanism covering the Lyra Basin but would also weaken the lithospheric keel
508 beneath it (Klosko et al., 2001). Alternatively, it is possible that the remanent heat due
509 to the thickness and volume of the OJP's lithospheric mantle root could have not
510 dissipated until after 34 Ma eruption of the alnoites. The reason why no heat anomaly
511 is detected at present may have been due to the finding that remanent heat may no
512 longer be geophysically detectable after 30 Ma cessation of active volcanism (Woods
513 and Okal., 1996).
514
515 **5. CONCLUSION**
516
517 The Lyra Basin lavas possess chemical and isotopic characteristics that are
518 distinct from those of the OJP tholeiites. Their isotopic compositions cannot be
519 directly related to any of the modern or Cretaceous Pacific hotspots that the plateau
520 might have crossed over on its way to its present location. Instead, the isotopic
521 composition of the Lyra Basin rocks that plots very close to those of the OJP data
522 fields in the isotope space is consistent with the involvement of the OJP lithospheric
523 mantle. Modeling suggests that the isotopic signature of the source of the basin lavas
524 can be explained by interaction of Rarotongan mantle-derived melts with the OJP
525 lithospheric mantle. Alternatively, the Lyra Basin basalts may be an expression of
526 relatively minor component in the OJP mantle source that remained isolated and
527 untapped until 65 Ma. Combined with other younger alkalic volcanism on the plateau,
528 the Lyra Basin basalts could represent part of the later stages in the hotspot
529 development of the OJP plume mantle.
530

ACKNOWLEDGMENTS

This paper is dedicated to the late Professor John Mahoney, a highly regarded mentor, friend, and one of the pioneers of LIPs study.

The Captain and Crew of R/V Kairei are appreciated for the successful implementation of the geophysical survey and dredging operations. K. Shimizu, T. Sano, and M. Nakanishi were supported by a Grant-in Aid fund from the Ministry of Education Science and Culture of Japan (Principal Investigator: Mike F. Coffin, No. 18340129) for travel fares. M. L. G. Tejada was able to carry out the Os-Hf isotope analytical work at JAMSTEC through support from Japan Society for the Promotion of Science Kakenhi Grant Nos. 20109006 and 20340158 to K. Suzuki and by a Special Detail from the University of the Philippines. We are grateful to the two anonymous reviewers and C. R. Neal for their critical comments and suggestions, which improved the manuscript considerably. B. S. Vaglarov, J-I. Kimura, and Y. Otsuki are appreciated for their assistance with the analytical work.

REFERENCES CITED

Agranier, A., Blichert-Toft, J., Graham, W.D., Debaille, V., Schiano, P., Albarede, F., 2005, The spectra of isotopic heterogeneities along the mid-Atlantic Ridge: Earth Planetary Science Letters, v. 238, p. 96-109.

Andres, M., Blichert-Toft, J., Schilling, J.G., 2002, Hafnium isotopes in basalts from *the* southern Mid-Atlantic Ridge from 40°S to 55°S: Discovery and Shona plume-ridge interactions and the role of recycled sediments: Geochemistry Geophysics Geosystems, v. 3, 8502, doi:10.1029/2002GC000324.

556 Bielski-Zyskind, M., Wasserburg, G.J., Nixon, P.H., 1984, Sm-Nd and Rb-Sr
557 systematics in volcanics and ultramafic xenoliths from Malaita, Solomon
558 Islands, and the nature of the Ontong Java Plateau: Journal of Geophysical
559 Research, v. 89, p. 2415-2424.
560 Birkhold-Van Dyke, A.L., Neal, C.R., Jain, J.C., Mahoney, J.J., and Duncan, R.A.,
561 1996, Multi-stage growth for the Ontong Java Plateau? A progress report from
562 San Cristobal (Makira): Abstract. Eos, Transactions of the American
563 Geophysical Union, v. 77, F714.
564 Bonneville, A., Dosso, L., Hildenbrand, A., 2006, Temporal evolution and
565 geochemical variability of the South Pacific superplume activity, Earth and
566 Planetary Science Letters, v. 244, 251-269.
567 Castillo, P.R., Carlson, R.W., and Batiza, R., 1991, Origin of Nauru Basin igneous
568 complex: Sr, Nd, and Pb isotopes and REE constraints: Earth and Planetary
569 Science Letters, v. 103, 200-213.
570 Castillo, P.R., Pringle, M.S., and Carlson, R.W., 1994, East Mariana Basin tholeiites:
571 Jurassic ocean crust or Cretaceous rift basalts related to the Ontong Java
572 plume?: Earth and Planetary Science Letters, v. 123, 139-154.
573 Castillo, P.R., Scarsi, P., Craig, H., 2007, He, Sr, Nd, and Pb isotopic constraints on
574 the origin of the Marquesas and other linear volcanic chains: Chemical
575 Geology, v. 240, 205-221.
576 Chandler, M.T., Wessel, P., Taylor, B., Seton, M., Seung-Sep, K., and Hyeong, K.,
577 *2012,* Reconstructing Ontong Java Nui: Implications for Pacific absolute plate
578 motion, hotspot drift and true polar wander: Earth and Planetary Science
579 Letters, v. 331-332, 140-151.

580 Chang, Q., Shibata, T., Shinotsuka, K., Yoshikawa, M., and Tatsumi, Y., 2002,
581 Precise determination of trace elements in geological standard rocks using
582 inductively coupled plasma mass spectrometry (ICP-MS): Frontier Research
583 on Earth Evolution, v. 1, p. 357-362.
584 Chauvel, C., and Blichert-Toft, J., 2001, A hafnium isotope and trace element
585 perspective on melting of the depleted mantle: Earth and Planetary Science
586 Letters, v. 190, p. 137-151.
587 Chen, C.-Y., Frey, F.A., Rhodes, J.M., and Easton, R.M., 1996, Temporal
588 geochemical evolution of Kilauea volcano: comparison of Hilina and Puna
589 basalt, *in* Basu, A.R., and Hart, S., eds., Earth Processes: Reading the Isotopic
590 Code: American Geophysical Union Geophysical Monograph 95, p. 161-181.
591 Cohen, R.S., Waters, F.G., 1996. Separation of osmium from geological materials by
592 solvent extraction for analysis by thermal ionization mass spectrometry. Anal.
593 Chim. Acta 332, 269-275.
594 Debaille, V., Blichert-Toft, J., Agranier, A., Doucelance, R., Schiano, P., Albarede,
595 F., 2006, Geochemical component relationships in MORB from the Mid-
596 Atlantic Ridge, 22-358N: Earth and Planetary Science Letters, v. 241, p. 844-
597 862.
598 Devey, C.W., Lackschewitz, K.S., Mertz, D.F., Bourdon, B., Cheminee, J.-L., Dubois,
599 J., Guivel, C., Hekinian, R., Stoffers, P., 2003, Giving birth to hotspot
600 volcanoes: Distribution and composition of young seamounts from the
601 seafloor near Tahiti and Pitcairn islands: Geology, v. 31, 395-398.
602 Eisele, J., Sharma, M., Galer, S.J.G., Blichert-Toft, J., Devey, C.W., Hoffman, A.W.,
603 2002, The role of sediment recycling in EM-1 inferred from Os, Pb, Hf, Nd, Sr

isotope and trace element systematics of the Pitcairn hotspot: Earth and Planetary Science Letters, v. 196, p. 197-212.

Escrig, S., Capmas, F., Dupre, B., Allegre, J.C., 2004, Osmium isotopic constraints on the nature of the DUPAL anomaly from Indian mid-ocean ridge basalts: Nature, v. 431, p. 59-63.

Fitton, J.G. and Godard, M., 2004, Origin and evolution of magmas on the Ontong Java Plateau, *in* Fitton, J.G., Mahoney, J.J., Wallace, P.J. and Saunders, A.D., eds., Origin and Evolution of the Ontong Java Plateau: Geological Society of London Special Publication 229, p. 151-178.

Garcia, M.O., Rhodes, J.M., Trusdell, F.A., and Pietruszka, A.J., 1996, Petrology of lavas from Puu Oo eruption of Kilauea volcano: III. The Kupaihana episode (1986-1992): Bulletin of Volcanology, v. 58, p. 359-379.

Gladczenko, T.P., Coffin, M.F., and Eldholm, O., 1997, Crustal structure of the Ontong Java Plateau: modeling of new gravity and existing seismic data: Journal of Geophysical Research, v. 102, p. 22,711- 22,729.

Hamelin, C., Dosso, L., Hanan, B., Moreira, M., Kositsky, A.P., Thomas, M.Y., 2011, Geochemical portray of the Pacific Ridge: New isotopic data and statistical techniques: Earth and Planetary Science Letters, v. 302, p. 154-162.

Hanyu, T., Nakai, S., Tatsuta, R., 2005, Hafnium isotope ratios of nine GSJ reference samples: Geochemical Journal, v. 39, p. 83-90.

Hanyu, T., Tatsumi, Y., Senda, R., Miyazaki, T., Chang, Q., Hirahara, Y., Takahashi, T., Kawabata, H., Suzuki, K., Kimura, J-I., Nakai, S., 2011, Geochemical characteristics and origin of the HIMU reservoir: A possible mantle plume source in the lower mantle: Geochemistry, Geophysics, Geosystems, v. 12, Q0AC09, doi:10.1029/2010GC003252.

629 Hart, S.R., Coetze, M., Workman, R.K., Blusztajn, J., Johnson, K.T. M., Sinton, J.M.,
630 Steinberger, B., Hawkins, J.W., 2004, Genesis of the Western Samoa
631 seamount province: age, geochemical fingerprint and tectonics: Earth and
632 Planetary Science Letters, v. 227, p. 37-56.
633 Hauri, E.H. and Hart, S.R., 1993, Re-Os isotope systematics of HIMU and EMII
634 oceanic island basalts from the south Pacific Ocean: Earth and Planetary
635 Science Letters, v. 114, p. 353-371.
636 Hirahara, Y., Takahashi, T., Miyazaki, T., Vaglarov, B.S., Chang, Q., Kimura, J-I.,
637 Tatsumi, Y., 2009, Precise Nd isotope analysis of igneous rock using cation
638 exchange chromatography and thermal ionization mass spectrometry (TIMS):
639 JAMSTEC Report of Research and Development Special Issue, p. 65-71.
640 Hirahara, Y., Chang, Q., Miyazaki, T., Takahashi, T. and Kimura, J.-I., 2012,
641 Improved Nd chemical separation technique for $^{143}Nd/^{144}Nd$ analysis in
642 geological samples using packed Ln resin columns: JAMSTEC Report of
643 Research and Development, v. 15, p. 27-33.
644 Hoernle, K., Hauff, F., van den Bogaard, P., Werner, R., Mortimer, N., Geldmacher,
645 J., Garbe-Schonberg, D., Davy, B., 2010, Age and geochemistry of volcanic
646 rocks from the Hikurangi and Manihiki oceanic Plateaus. Geochimica et
647 Cosmochimica Acta, v. 74, p. 7196-7219.
648 Ingle, S. and Coffin, M., 2004, Impact origin for the greater Ontong Java Plateau?:
649 Earth and Planetary Science Letters, v. 218, p. 123-134.
650 Ingle, S., Mahoney, J.J., Sato, H., Coffin, M.F., Kimura, J-I., Hirano, N., and
651 Nakanishi, M., 2007, Depleted mantle wedge and sediment fingerprint in
652 unusual basalts from the Manihiki Plateau, central Pacific Ocean: Geology, v.
653 35, p. 595-598.

654 Ishikawa, A., Maruyama, S., Komiya, T., 2004, Layered lithospheric mantle beneath
655 the Ontong Java Plateau: implications from xenoliths in alnöite, Malaita,
656 Solomon Islands: Journal of Petrology, v. 45, p. 2011-2044.
657 Ishikawa, A., Nakamura, E., Mahoney, J.J., 2005, Jurassic oceanic lithosphere
658 beneath the southern Ontong Java Plateau: evidence from xenoliths in alnöite,
659 Malaita, Solomon Islands: Geology, v. 33, p. 393-396.
660 Ishikawa, A., Kuritani, T., Makishima, A., Nakamura, E., 2007, Ancient recycled
661 crust beneath the Ontong Java Plateau: Isotopic evidence from the garnet
662 clinopyroxenite xenoliths, Malaita, Solomon Islands: Earth and Planetary
663 Science Letters, v. 259, p. 134-148.
664 Ishikawa, A., Pearson, D., Dale, C.W., 2011, Ancient Os isotope signatures from the
665 Ontong Java Plateau lithosphere: tracing lithospheric accretion history: Earth
666 and Planetary Science Letters, v. 301, p. 159-170.
667 Jackson, M.G. and Shirey, S.B., 2011, Re-Os isotope systematics in Samoan shield
668 lavas and the use of Os-isotopes in olivine phenocryts to determine primary
669 magmatic compositions: Earth and Planetary Science Letters, v. 312, p. 191-
670 101.
671 Jackson, M.G., Kurz, M.D., Hart, S.R., and Workman, R.K., 2007, New Samoan
672 lavas from Ofu island reveal a hemispherically heterogeneous high $^{3}He/^{4}He$
673 mantle: Earth and Planetary Science Letters, v. 264, p. 360-374.
674 Jackson, M.G., Hart, S.R., Konter, J.G., Koppers, A.P., Staudigel, H., Kurz, M.D.,
675 Blusztajn, J., and Sinton, J.M., 2010, Samoan hot spot track on a “hot spot
676 highway”: Implications for mantle plumes and a deep Samoan mantle source:
677 Geochemistry, Geophysics, Geosystems, v. 11, Q12009, doi:10.1029/2010
678 GC003232.

679 Janney, P.E., Le Roex, A.P., Carlson, R.W., 2005, Hafnium isotopes and trace
680 element constraints on the nature of mantle heterogeneity beneath the central
681 Southwest Indian Ridge (13^{o}E to 47^{o}E): Journal of Petrology, v. 46, p. 2427-
682 2464.
683 Kitajima, K., Ishikawa, A., Maruyama, S., and Sano, Y., 2008, Nano-SIMS U-Pb
684 zircons dating and geochemistry of alnöite in Malaita, Solomon Islands: 9th
685 International Kimberlite Conference, Extended Abstract No. 91K-A-00329.
686 Klosko, E.R., Russo, R.M., Okal, E.A., Richardson, W.P., 2001, Evidence for a
687 rheologically strong chemical mantle root beneath the Ontong Java Plateau:
688 Earth and Planetary Science Letters, v. 186, p. 347-361.
689 Konter, J.G., Hanan, B.B., Blichert-Toft, J., Koppers, A.P., Plank, T., and Staudigel,
690 H., 2008, One hundred million years of mantle geochemical history suggest
691 the retiring of mantle plumes is premature: Earth and Planetary Science
692 Letters, v. 275, p. 285-295.
693 Koppers, A.P., Staudigel, H., Pringle, M.S., Wijbrans, J.R., 2003, Short-lived and
694 discontinuous intraplate volcanism in the South Pacific: Hot spots or
695 extensional volcanism?: Geochemistry, Geophysics, Geosystems, v. 4, p.
696 1089, doi:10.1029/ 2003GC000533.
697 Koppers, A.P., Russell, J.A., Jackson, M.G., Konter, J., Staudigel, H., Hart, S., 2008,
698 Samoa reinstated as a primary hotspot trail, Geology, v. 36, 435-438.
699 Kroenke, L., 1972, Geology of the Ontong Java Plateau. Hawaii Institute of
700 Geophysics Report 72-75, University of Hawaii, 119 p.
701 Lassiter, J.C. and Hauri, E.H., 1998, Osmium-isotope variations in Hawaiian lavas:
702 evidence for recycled oceanic lithosphere in the Hawaiian plume: Earth and
703 Planetary Science Letters, v. 164, p. 483-496.

Lassiter, J.C., Blichert-Toft, J., Hauri, E.H., and Barsczus, H.G., 2003, Isotope and *trace* element variations in lavas from Raivaevae and Rapa, Cook-Austral islands: constraints on the nature of HIMU- and EM-mantle and the origin of mid-plate volcanism in French Polynesia: Chemical Geology, v. 202, p. 115-138.

Mahoney, J.J. and Spencer, K.J., 1991, Isotopic evidence for the origin of the Manihiki and Ontong Java oceanic plateaus: Earth and Planetary Science Letters, v. 104, p. 196-210.

Mahoney, J.J., Storey, M., Duncan, R.A., Spencer, K.J., Pringle, M., 1993, Geochemistry and geochronology of the Ontong Java Plateau, *in* Pringle, M., Sager, W., Sliter, W., and Stein, S., eds., The Mesozoic Pacific. Geology, Tectonics, and Volcanism: American Geophysical Union Geophysical Monograph Volume 77, p. 233-261.

Mahoney, J.J., Sinton, J.M., Macdougall, J.D., Spencer, K.J. and Lugmair, G.W., 1994, Isotope and trace element characteristics of a super-fast spreading ridge: East Pacific rise, 13–23ºS: Earth and Planetary Science Letters, v. 121, p. 173–193.

Miyazaki, T., Kanazawa, N., Takahashi, T., Hirahara, Y., Vaglarov, B.S., Chang, Q., Kimura, J-I., Tatsumi, Y., 2009, Precise Pb isotope analysis of igneous rocks using fully automated double spike thermal ionization mass spectrometry (FA-DS-TIMS): JAMSTEC Report of Research and Development Special Issue, p. 73-80.

Miyazaki, T., Vaglarov, B.S., Takei, M., Suzuki, M., Suzuki, H., Ohsawa, K., Chang, Q., Takahashi, T., Hirahara, Y., Hanyu, T., Kimura, J.-I., Tatsumi, Y., 2012, Development of a fully automated open-column chemical-separation system—

729 COLUMNSPIDER— and its application to Sr-Nd-Pb isotope analyses of
730 igneous rock samples: Journal of Mineralogical and Petrological Sciences, v.
731 107, p. 74-86.
732 Mochizuki, K., Coffin, M.F., Eldholm, O., and Taira, A., 2005, Massive Early
733 Cretaceous volcanic activity in the Nauru Basin related to emplacement of the
734 Ontong Java Plateau: Geochemistry, Geophysics, Geosystems, v. 6, Q10003,
735 doi:10.1029/2004GC000867.
736 Nakamura, Y. and Tatsumoto, M., 1988, Pb, Nd, and Sr isotopic evidence for a
737 multicomponent source for rocks of Cook-Austral Islands and heterogeneities
738 of mantle plumes: Geochimica et Cosmochimica Acta, v. 52, p. 2909-2924.
739 Nakanishi, M., Sano, T., Shimizu, K., 2007, Tectonic setting of the Lyra Basin, west
740 of the Ontong Java Plateau: American Geophysical Union Fall Meeting 2007,
741 Abstract T13A-1122.
742 Natland, J. H., 1985, The Samoa-Malaita connection: Eos, Transactions, American
743 Geophysical Union, v. 66, p. 1080.
744 Neal, C.R., and Davidson, J.P., 1989, An unmetasomatized source for the Malaitan
745 alnoite (Solomon Islands): Petrogenesis involving zone refining, megacryst
746 fractionation, and assimilation of oceanic lithosphere: Geochimica et
747 Cosmochimica Acta, v. 55, p. 1975-1990.
748 Neal, C. R., Mahoney, J. J., Kroenke, L. W., Duncan, R. A., and Petterson, M. G.,
749 1997, The Ontong Java Plateau, *in* Mahoney, J. J., and Coffin, M., eds., Large
750 Igneous Provinces: American Geophysical Union Geophysical Monograph
751 Series 100, p. 183-216.

O'Neill, C., Muller, D., Steinberger, B., 2005, On the uncertainties in hot spot reconstructions and the significance of moving hot spot reference frames: Geochemistry, Geophysics, Geosystems, v. 6, p. 1-35.

Palacz, Z., and Saunders, A.D., 1986, Coupled trace element and isotope enrichment *on* the Cook-Austral-Samoa Islands, southwest Pacific: Earth and Planetary Science Letters, v. 79, p. 270-280.

Patchett, P.J. and Tatsumoto, M., 1980, Hafnium isotope variations in oceanic basalts: Geophysical Research Letters, v. 7, p. 1077-1080.

Pearson, D.G., Woodland, S.J., 2000. Solvent extraction/anion exchange separation and determination of PGEs (Os, Ir, Pt, Pd, Ru) and Re-Os isotopes in geological samples by isotope dilution ICP-MS. Chem. Geol. 165, 87-107.

Petterson, M.G., Neal, C.R., Mahoney, J.J., Kroenke, L., Saunders, A.D., Babbs, T.L., Duncan, R.A., Tolia, D., McGrail, B., 1997, Structure and deformation of north and central Malaita, Solomon Islands: tectonic implications for the Ontong Java Plateau-Solomon arc collision, and for the fate of oceanic plateaus: Tectonophysics, v. 283, p. 1-33.

Rhodes, J.M. and Hart, S.R., 1995, Evolution of Mauna Loa volcano: episodic trace element and isotopic variations in historical Mauna Loa lavas: implications for magma and plume dynamics, *in* Rhodes, J.M., and Lockwood, J.P., eds., Mauna Loa Revealed: Structure, Composition, History, and Hazards: American Geophysical Union Geophysical Monograph Volume 92, p. 263-288.

Richardson, W.P., Okal, E.A., and Van der Lee, S., 2000, Rayleigh-wave tomography of the Ontong Java Plateau: Physics of the Earth and Planetary Interiors, v. 118, p. 29-61.

777 Roden, M.F., Trull, T., Hart, S.R., and Frey, F.A., 1994, New He, Nd, Pb, and Sr
778 isotopic constraints on the constitution of the Hawaiian plume: results from
779 Koolau Volcano, Oahu, Hawaii, USA: Geochimica et Cosmochimica Acta, v.
780 58, p. 1431-1440.
781 Roy-Barman, M. and Allegre, C.J., 1995. $^{187}Os/^{186}Os$ in oceanic island basalts:
782 *tracing* oceanic crust recycling in the mantle. Earth Planet. Sci. Lett. 129, 145-
783 161.
784 Saunders, A. D., 1986, Geochemistry of basalts from the Nauru Basin, Deep Sea
785 Drilling Project Legs 61 and 89: Implications for the origin of oceanic flood
786 basalts, in Moberly, R., Schlanger, S. O. et al., Initial Report of the Deep Sea
787 Drilling Project Volume 89: Washington D. C., U.S. Government Printing
788 Office, p. 499-518.
789 Schiano, P., Birck, J.-L., Allegre, C.J., 1997, Osmium-strontium-neodymium-lead
790 isotopic variations in mid-ocean ridge basalt glasses and the heterogeneity of
791 the upper mantle: Earth and Planetary Science Letters, v. 150, p. 363-379.
792 Schiano, P., Burton, K.W., Dupre, B., Birck, J.-L., Guille, G., and Allegre, C.J., 2001,
793 Correlated Os-Pb-Nd-Sr isotopes in the Austral-Cook chain basalts: the nature
794 of mantle components in plume sources: Earth and Planetary Science Letters,
795 v. 186, p. 527-537.
796 Shimizu, K. Sano, T., Tejada, M.L.G., Hyodo, H., Sato, K., Suzuki, K., Chang, Q.,
797 Nakanishi, M., 2014, Alkalic magmatism in the Lyra Basin: A missing link in
798 the evolution of the Ontong Java Plateau: this volume.
799 Shimoda, G., Ishizuka, O., Yamashita, K., Yoshitake, M., Ogasawara, M., and Yuasa,
800 *M.,* 2011, Tectonic influence on chemical composition of ocean island basalts
801 in the West and South Pacific: Implications for a deep mantle origin:

802 Geochemistry, Geophysics, Geosystems, v. 12, Q07020, doi:10.1029/
803 2011GC003531.
804 Simonetti, A., and Neal, C.R., 2010, In-situ chemical, U-Pb dating, and Hf isotope
805 investigation of megacrystic zircons, Malaita (Solomon Islands): Evidence for
806 multi-stage alkaline magmatic activity beneath the Ontong Java Plateau: Earth
807 and Planetary Science Letters, v. 295, p. 251-261.
808 Smith, W.H.F., and Sandwell, D.T., 1997, Global seafloor topography from satellite
809 altimetry and ship depth soundings: Science, v. 277, p. 1956-1962.
810 Stille, P., Unruh, D.M., Tatsumoto, M., 1986, Pb, Sr, Nd, and Hf isotopic constraints
811 on the origin of Hawaiian basalts and evidence for a unique mantle source:
812 Geochimica et Cosmochimica Acta, v. 50, p. 2303-2319.
813 Suzuki, K., Miyata, Y., Kanazawa, N., 2004, Precise Re isotope ratio measurements
814 by negative thermal ionization mass spectrometry (N-TIMS) using total
815 evaporation technique: International Journal of Mass Spectrometry, v. 235, p.
816 97-101.
817 Takahashi, T., Hirahara, Y., Miyazaki, T., Vaglarov, B. S., Chang, Q., Kimura, J-I.,
818 Tatsumi, Y., 2009, Precise determination of Sr isotope ratios in igneous rock
819 samples and application to micro-analysis of plagioclase phenocrysts:
820 JAMSTEC Report of Research and Development Special Issue, p. 59-64.
821 Tanaka, T., Togashu, S., Kamioka, H., Amakawa, H., Kagami, H., Hamamoto, T.,
822 Yuhara, M., Orihashi, Y., Yoneda, S., Shimizu, H., Kunimaru, T., Takahashi,
823 K., Yanagi, T., Nakano, T., Fujimaki, H., Shinjo, R., Asahara, Y., Tanimizu,
824 M., Draguzano, C., 2000, J-Ndi: a neodymium isotopic reference in
825 consistency with La Jolla neodymium: Chemical Geology, v. 168, p. 279-281.

826 Tatsumoto, M., 1978, Isotopic composition of lead in oceanic basalt and its
827 implication *to* mantle evolution: Earth and Planetary Science Letters, v. 38, p.
828 63-87.
829 Taylor, B., 2006, The single largest oceanic plateau: Ontong Java-Manihiki-
830 Hikurangi*:* Earth and Planetary Science Letters, v. 241, p. 372-380.
831 Tejada, M.L.G., Mahoney, J.J., Duncan, R.A., and Hawkins, M.P., 1996, Age and
832 geochemistry of basement and alkalic rocks of Malaita and Santa Isabel,
833 Solomon Islands, southern margin of Ontong Java Plateau: Journal of
834 Petrology*,* v. 37, p. 361-394.
835 Tejada, M.L.G., Mahoney, J.J., Neal, C.R., Duncan, R.A., and Petterson, M.G., 2002,
836 Basement geochemistry and geochronology of Central Malaita, Solomon
837 Islands, with implications for the origin and evolution of the Ontong Java
838 Plateau: Journal of Petrology, v. 43, p. 449-484.
839 Tejada, M.L.G., Mahoney, J.J., Castillo, P.R., Ingle, S.P., Sheth, H.C., and Weis, D.,
840 2004, Pin-pricking the elephant: Evidence on the origin of the Ontong Java
841 Plateau from Pb-Sr-Hf-Nd isotopic characteristics of ODP Leg 192 basalts: *in*
842 Fitton, J.G. et al., eds., Origin and Evolution of the Ontong Java Plateau:
843 Geological Society of London Special Publication 229, p. 133-150.
844 Tejada, M.L.G., Suzuki, K., Hanyu, T., Mahoney, J.J., Ishikawa, A., Tatsumi, Y.,
845 Chang, Q. and Nakai, S., 2013, Cryptic lower crustal signature in the source of
846 the Ontong Java Plateau revealed by Os and Hf isotopes: Earth and Planetary
847 Science Letters 377-378, 84-96.
848 Timm, C., Hoernle, K., Werner, R., Hauff, F., van den Bogaard, P., Michael, P.,
849 Coffin*,* M.F., and Koppers, A., 2011, Age and geochemistry of the oceanic

Manihiki Plateau, SW Pacific: New evidence for a plume origin: Earth and Planetary Science Letters, v. 304, p. 135-146.

Vidal, P., Chauvel, C., and Brousse, R., 1984, Large mantle heterogeneity beneath French Polynesia: Nature, v. 307, p. 536-538.

Wessel, P., and Kroenke, L.W., 2008, Pacific absolute plate motion since 145 Ma: an assessment of the fixed hot spot hypothesis: Journal of Geophysical Research, v. 113, p. 1-21.

White, W.M., and Hoffman, A.W., 1982, Sr and Nd isotope geochemistry of oceanic basalts and mantle evolution: Nature, v. 296, p. 821-825.

White, W. M., Hoffman, A. W. and Puchelt, H., 1987. Isotope geochemistry of Pacific mid-ocean ridge basalt. Journal of Geophysical Research 92, 4881-4893.

Woodhead, J.D. and Devey, C.W., 1993, Geochemistry of the Pitcairn seamounts, I: source character and temporal trends: Earth and Planetary Science Letters, v. 116, p. 81-99.

Woods, M.T., and Okal, E.A., 1996, Rayleigh-wave dispersion along the Hawaiian Swell; a test of lithospheric thinning by thermal rejuvenation at a hotspot: Geophysical Journal International, v.125, p. 325-339.

Wright, E., and White, W. M., 1987, The origin of Samoa: new evidence from Sr, Nd, and Pb isotopes: Earth and Planetary Science Letters, v. 81, p. 151-162.

Yan, C., Y., and Kroenke, L., 1993, A plate tectonic reconstruction of the southwest Pacific, 0-100 Ma, *in* Berger, W. H., Kroenke, L. W., Mayer, L. A., et al. (eds.) Scientific Results, Ocean Drilling Program, Leg 130: College Station, Texas Ocean Drilling Program, p. 697-710.

875 **FIGURE CAPTIONS**

876

877 **Figure 1. a)** Location of three major oceanic plateaus in the Pacific Ocean, Ontong
878 Java Plateau (OJP), Manihiki Plateau (MP), and Hikurangi Plateau (HP), suggested by
879 Taylor (2006) and Chandler et al. (2012) to be fragments of one very large oceanic
880 plateau. The box shows the location of the map area in b. **b)** A more detailed map
881 showing the area surveyed by R/V Kairei Cruise KR06-16 on the Lyra Basin, which
882 is shown in detail in Fig. 2. The maps are modified from Taylor (2006) and from the
883 satellite-derived bathymetry maps of Smith and Sandwell (1997).

884

885 **Figure 2.** Survey area showing the location of dredges D1 and D2. D1 is to the west
886 and is on one side of the ridge and D2 is along a fault scarp to the east at the base of
887 one of the seamounts dotting the eastern margin of the basin.

888

889 **Figure 3.** Total alkali vs. SiO_2 (top) and Nb vs. Zr (bottom) plots for basaltic rocks of
890 Lyra Basin in comparison with data for OJP tholeiites and alkalic rocks from Malaita
891 and Santa Isabel, Solomon Islands. Data for OJP and alkalic rocks are from Tejada et
892 al. (1996; 2002) and Fitton and Goddard (2004). Modified from Fitton and Godard
893 (2004).

894

895 **Figure 4.** Initial ε_{Nd} vs. initial $^{87}Sr/^{86}Sr$ **(a)** and initial $^{206}Pb/^{204}Pb$ **(b)** for Lyra Basin
896 alkalic rocks. Data points for Santa Isabel and Malaitan alkalic rocks (Tejada et al.,
897 1996) and Malaitan alnoites and pyroxenite xenoliths (Ishikawa et al., 2005; 2007) are
898 also plotted. Data fields for OJP tholeiites (Mahoney et al., 1993; Tejada et al., 1996;
899 2002; 2004), Mahiniki Plateau (Mahoney and Spencer, 1991; Ingle et al., 2007;

Hoernle et al., 2010; Timm et al., 2011), Pacific MORB (White *et al.,* 1987; Mahoney *el al.,*1994, and references therein; Hamelin et al., 2011), and selected Pacific OIB fields: Hawaii (Tatsumoto, 1978; Stille et al., 1986; Roden et al., 1994; Rhodes and Hart, 1995; Chen et al., 1996; Garcia et al., 1996; Lassiter and Hauri, 1998); Rarotonga (Palacz & Saunders, 1986; Nakamura & Tatsumoto, 1988; Schiano et al., 2001; Hanyu et al, 2011), Samoan shields (Wright & White, 1987; Hart et al., 2004; Jackson et al., 2007; 2010); and Mangaia Group (Vidal *el al.,* 1984; Palacz & Saunders, 1986; Nakamura & Tatsumoto, 1988; Hauri & Hart, 1993; Hanyu et al., 2011) are shown for reference. The field for Malaitan alnoite in panel (a) is from Bielski-Zyskind et al. (1984) and Neal & Davidson (1989). The dashed data fields are estimates of age-corrected Samoan and Rarotongan data at 65 Ma. The rest are estimated positions of mantle sources at 120 Ma (gray field for Pacific MORB). Errors for data of this study are similar to or smaller than the size of the symbols.

Figure 5. $(^{206}Pb/^{204}Pb)_t$ vs. $(^{208}Pb/^{204}Pb)_t$ **(a)** and $(^{207}Pb/^{204}Pb)_t$ **(b)** for Lyra Basin alkalic rocks. Data points for Santa Isabel and Malaita alkalic rocks, as well as for Malaitan alnoites and pyroxenites are plotted for comparison. The other data fields from Fig. 4 are also shown for reference. Data sources are as in Fig. 4. Errors for data of this study are similar to or smaller than the size of the symbols.

Figure 6. $\varepsilon_{Hf}(t)$ vs. $\varepsilon_{Nd}(t)$ **(a)** and $(^{187}Os/^{188}Os)_t$ **(b)** for Lyra Basin alkalic rocks. Data points for Malaitan alnoites and pyroxenite xenoliths (Ishikawa et al., 2005; 2007; 2011) are also plotted. Data fields for Pacific, Atlantic, and Indian MORBs (Schiano et al., 1997; Chauvel and Blichert-Toft, 2001; Andres et al., 2002; Escrig et al., 2004; Janney et al., 2005; Agranier et al., 2005; Debaille et al., 2006; Hamelin et al.,

925 2011and *PetDB* database), OJP (Tejada et al., 2004; 2013); Manihiki Plateau (Timm
926 et al., 2011); Pitcairn lavas (Eisele et al., 2002), Samoa (Patchett and Tatsumoto,
927 1980; White and Hoffman, 1982; Jackson and Shirey, 2011), and Rarotonga (Hanyu
928 et al., 2011) are also shown for reference. The box for Samoan data indicates only a
929 range in $^{187}Os/^{188}Os$ because the samples with available Os data are not the same ones
930 with Nd and Hf isotope data.
931
932 **Figure 7.** Reconstructions of the OJP's path from 125 Ma to its present location
933 shown as flowlines based on Wessel and Kroenke (2008; blue) and O'Neill et al.
934 (2005; green) Pacific absolute plate motion (modified from Chandler et al., 2012).
935 The present-day locations of selected Polynesian hotspots are shown for reference.
936 RA and MG refer to Rarotonga and Mangaia hotspot locations, respectively.
937
938 **Figure 8.** Bivariate plots of $(^{206}Pb/^{204}Pb)_t$, $(^{187}Os/^{188}Os)_t$, $\varepsilon_{Hf}(t)$ and $\varepsilon_{Nd}(t)$ comparing
939 the Lyra Basin data with model curves (solid curve with + markers) derived by
940 mixing of Kroenke-type basalt composition, representing OJP lithospheric mantle
941 source, with Rarotonga melt composition. The OJP source is assumed to have evolved
942 isotopically from 120 Ma to 65 Ma before reaction with the Rarotongan melt whose
943 composition is estimated from the present-day and assumed ~95 Ma data from the
944 same hotspot. See Table 4 caption for data sources and model parameters.
945
946

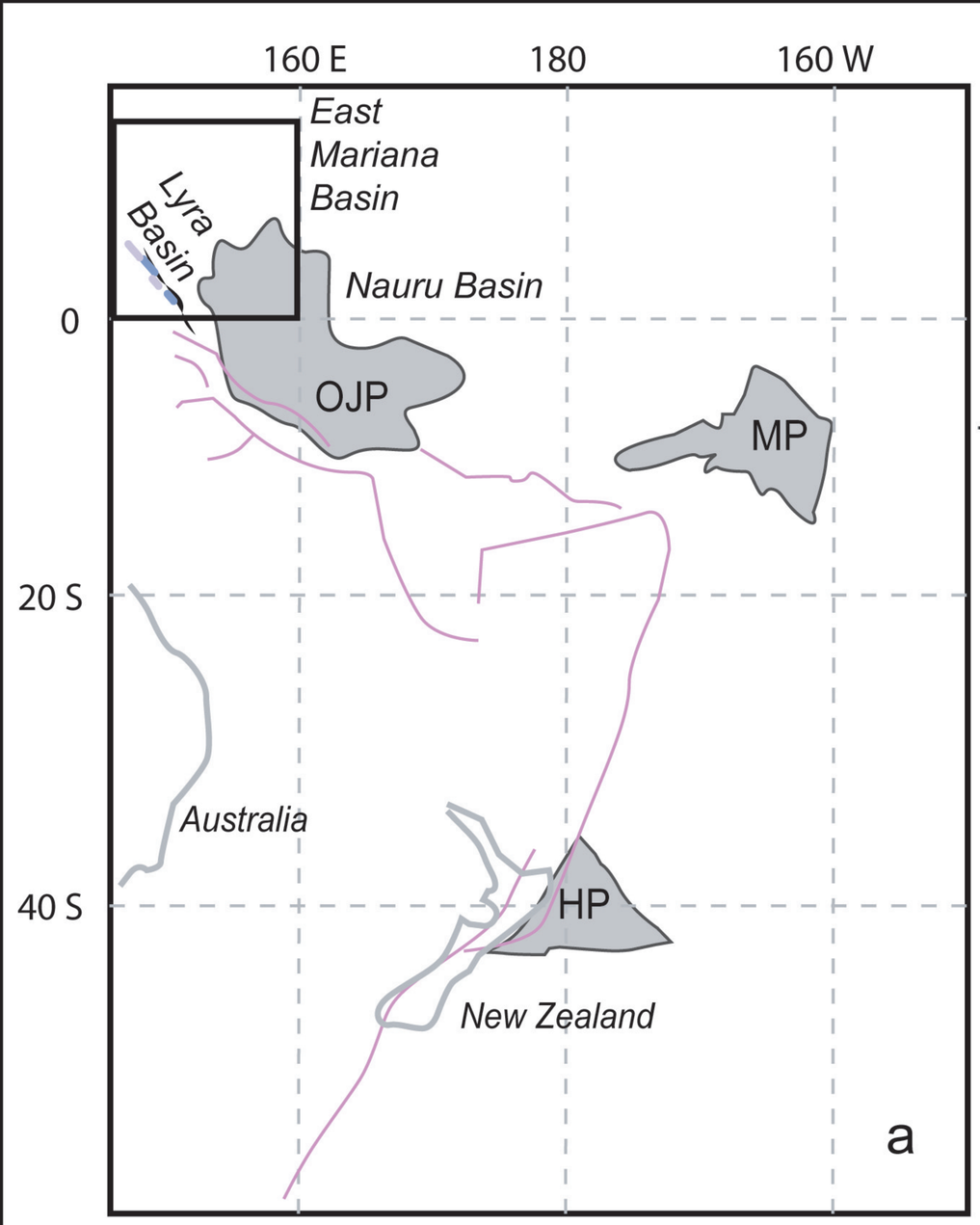

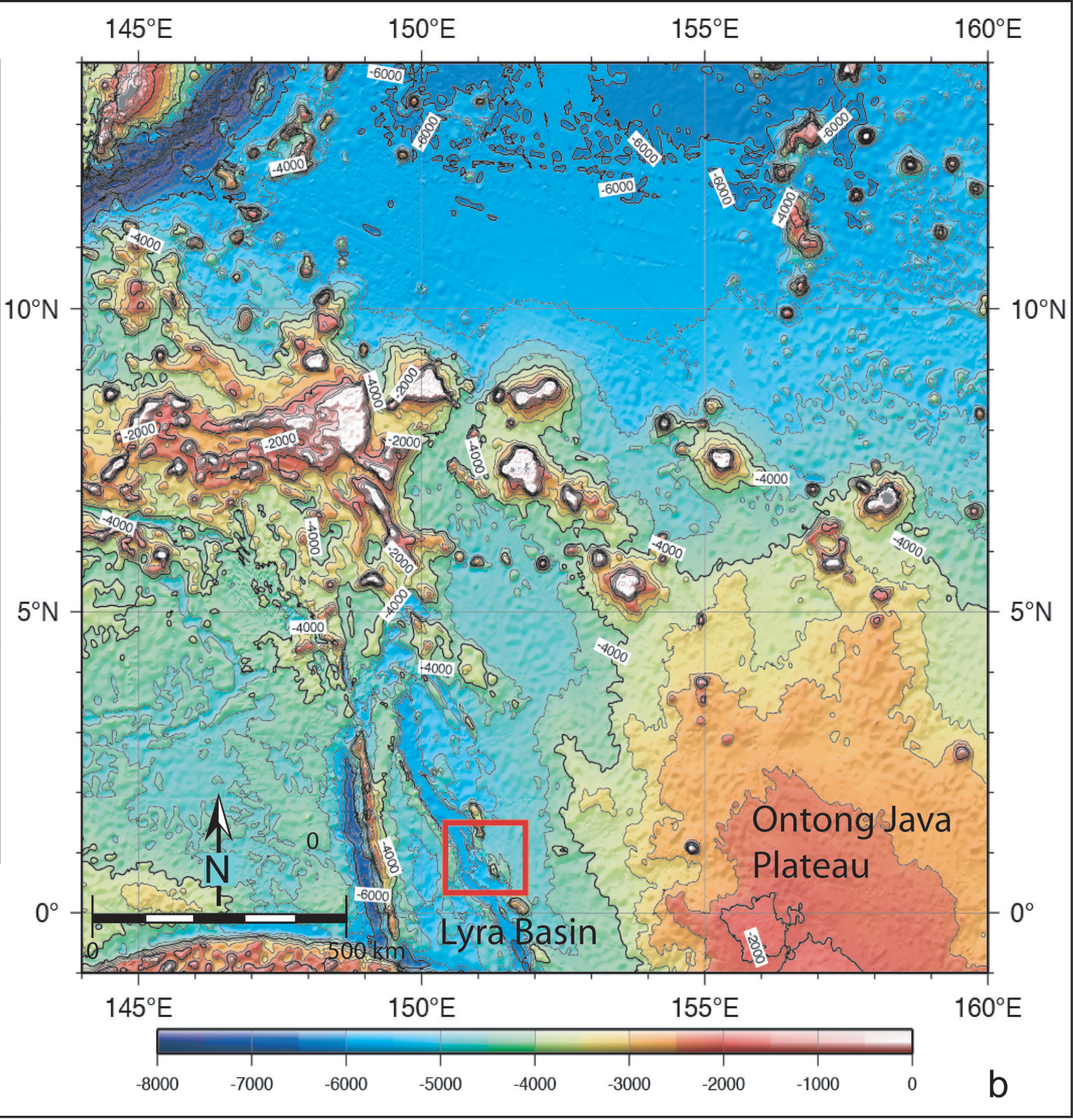

Figure 1, Tejada et al. 2014

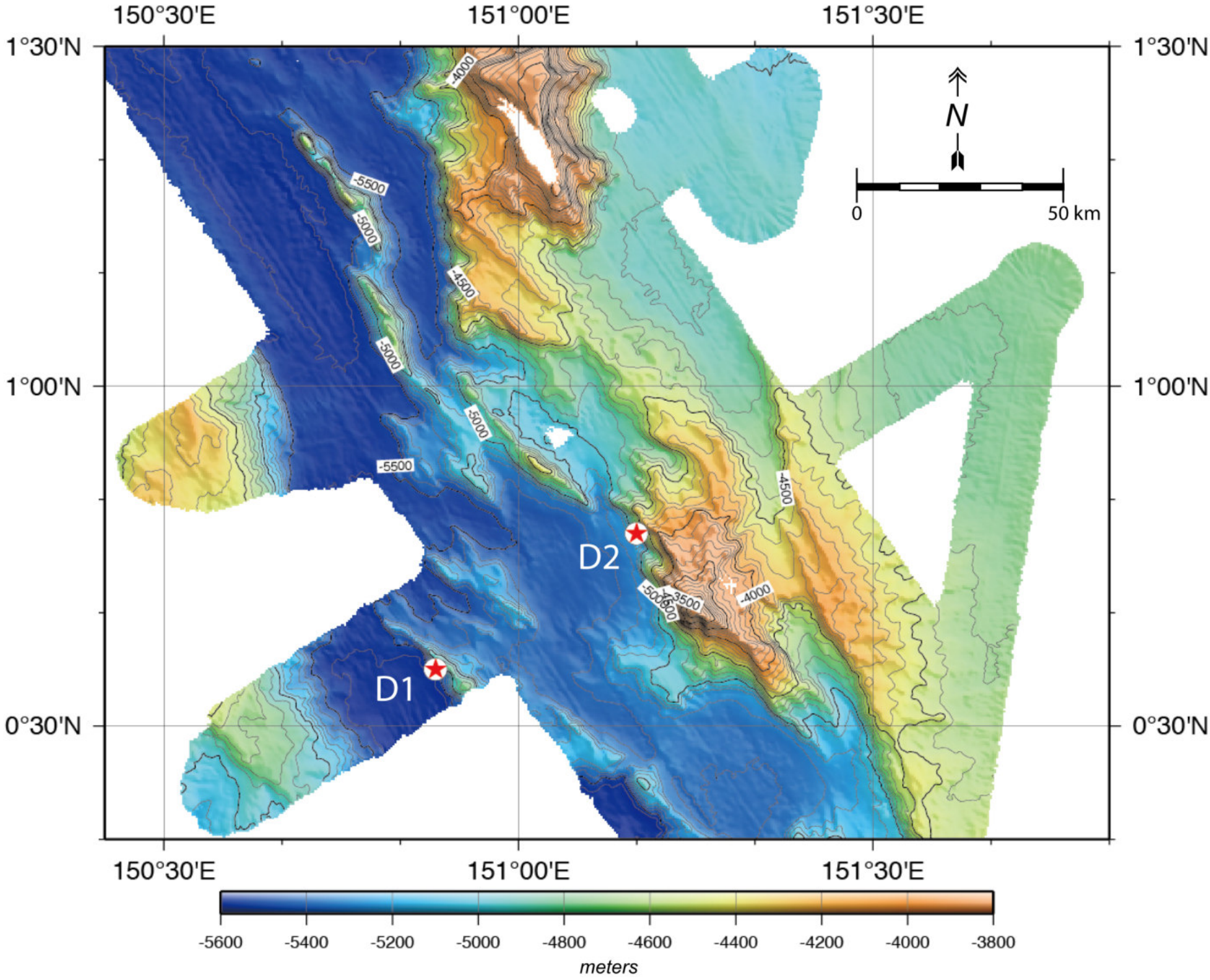

Figure 2, Tejada et al. 2014

a

Trachy-andesite

Tephrite

ALKALINE

THOLEIITIC

Basaltic trachy-andesite

Trachy-basalt

Basanite

Andesite

OJP

Basaltic andesite

Picro-basalt

Basalt

Na_2O+K_2O, wt%

SiO_2, wt%

Younger Series

N. Malaita Alk.

Sigana Alkalic

Lyra Basin

Alnoite, average

OIB

OJP

NMORB

Iceland

b

Nb

Zr

Figure 3, Tejada et al. 2014

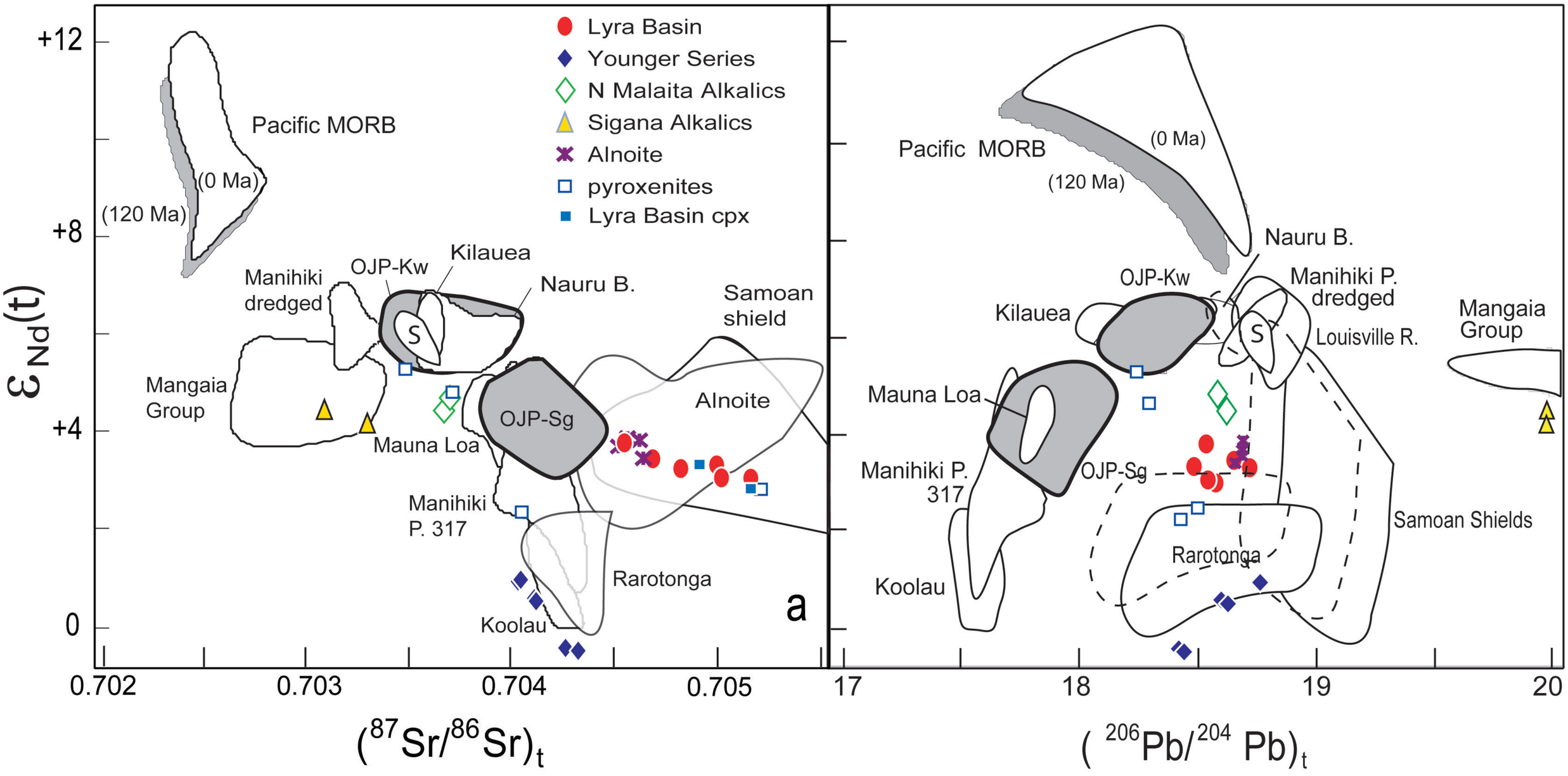

Figure 4, Tejada et al. 2014

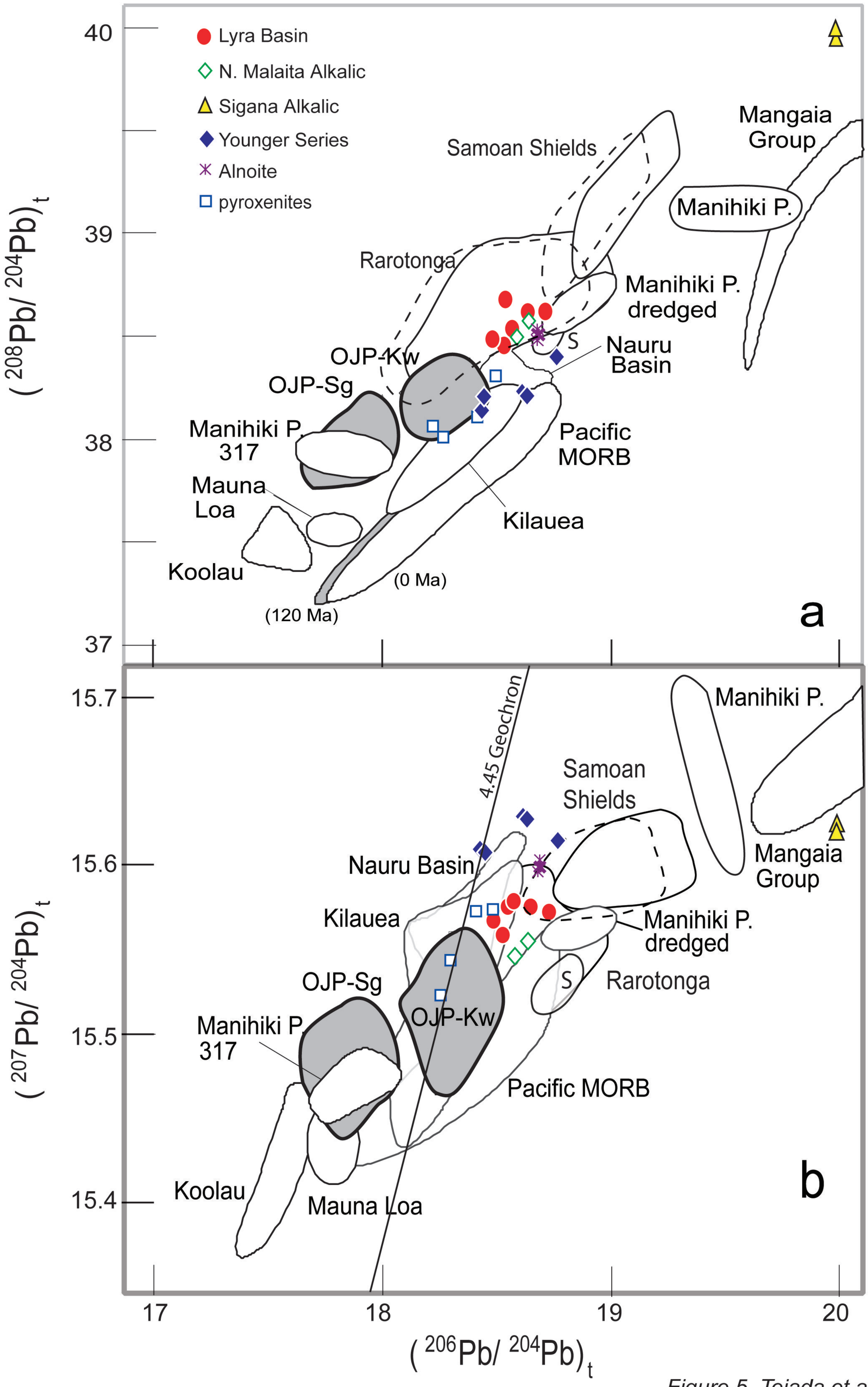

Figure 5, Tejada et al. 2014

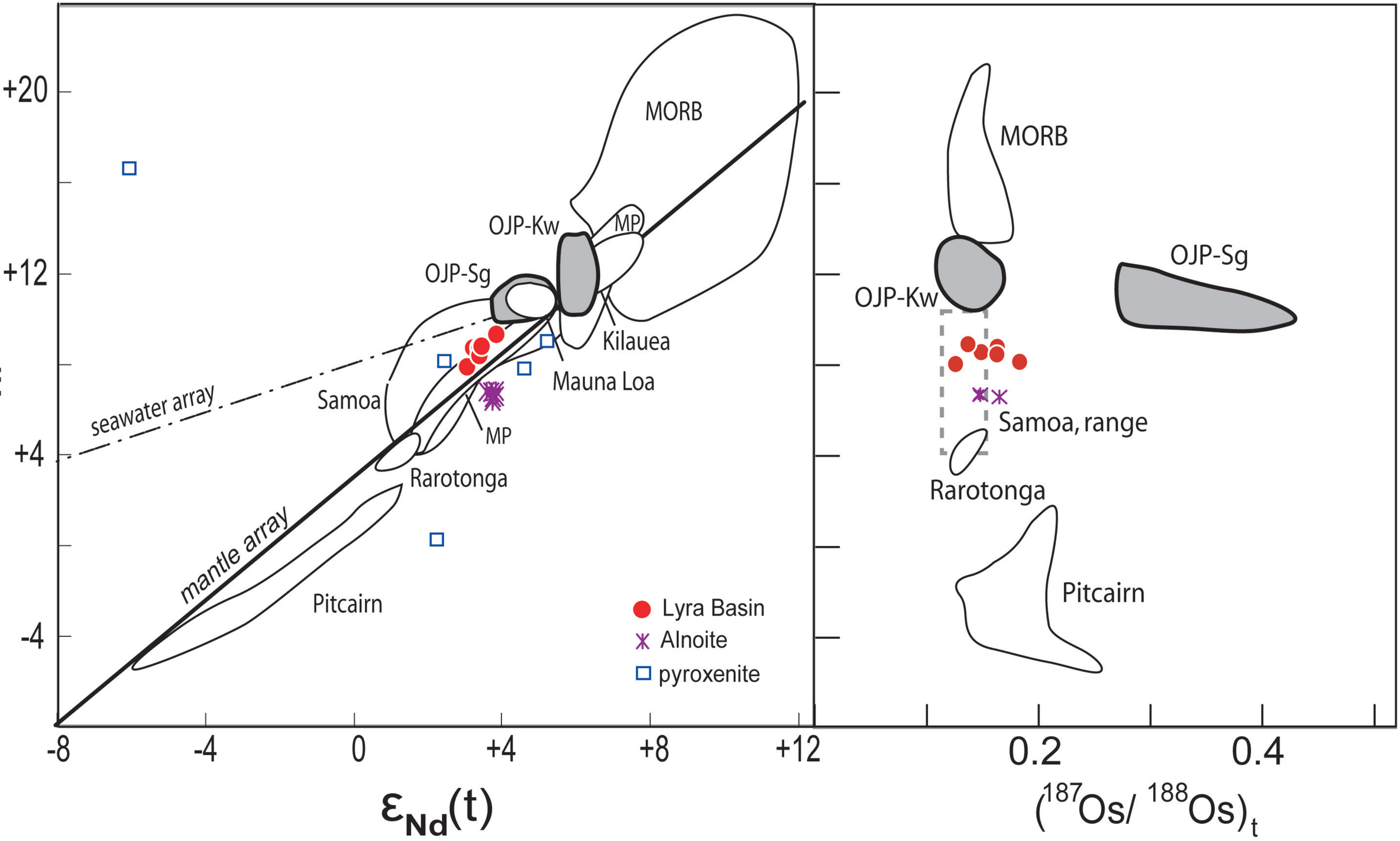

Figure 6, Tejada et al. 2014

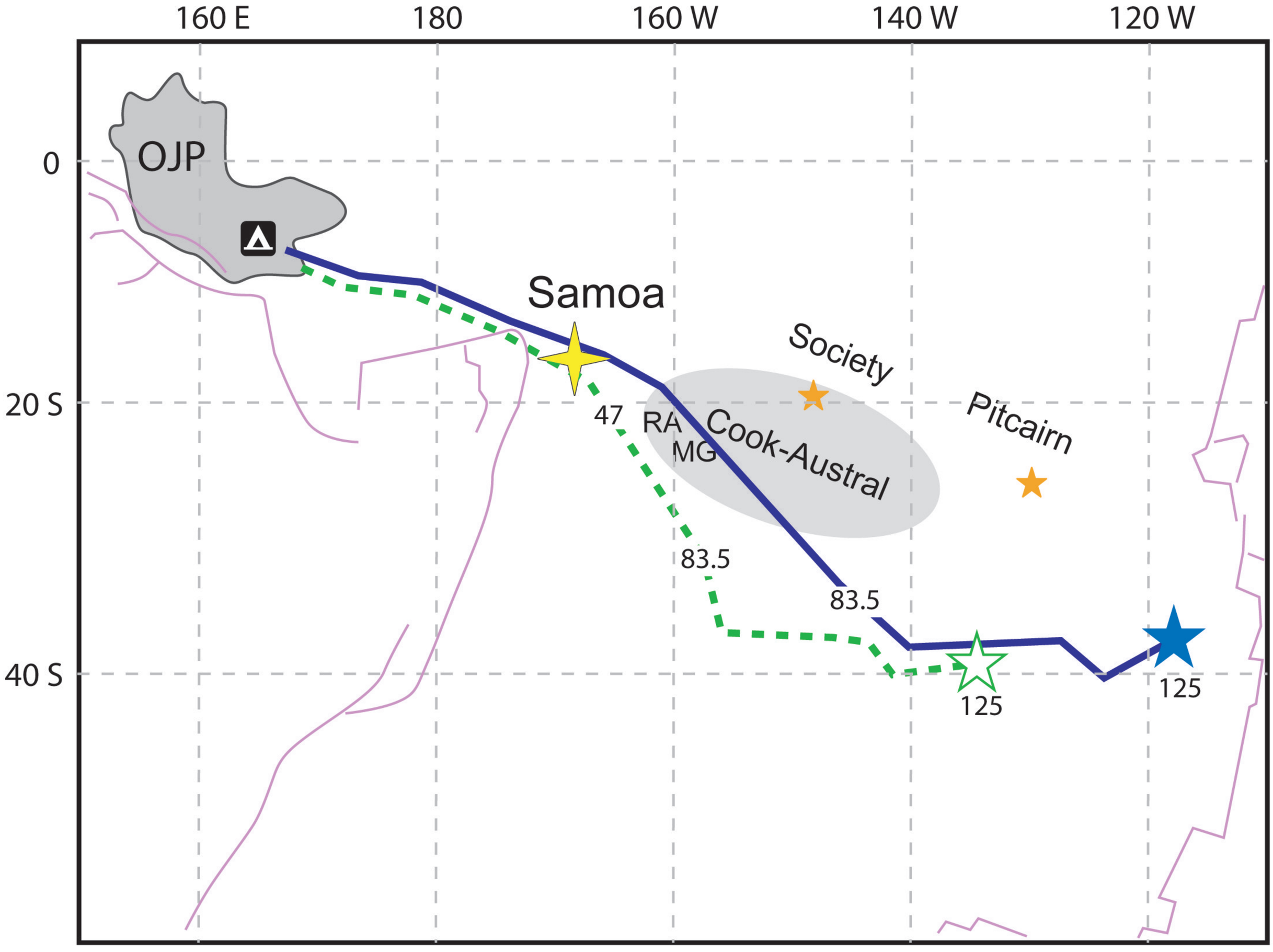

Figure 7, Tejada et al. 2014

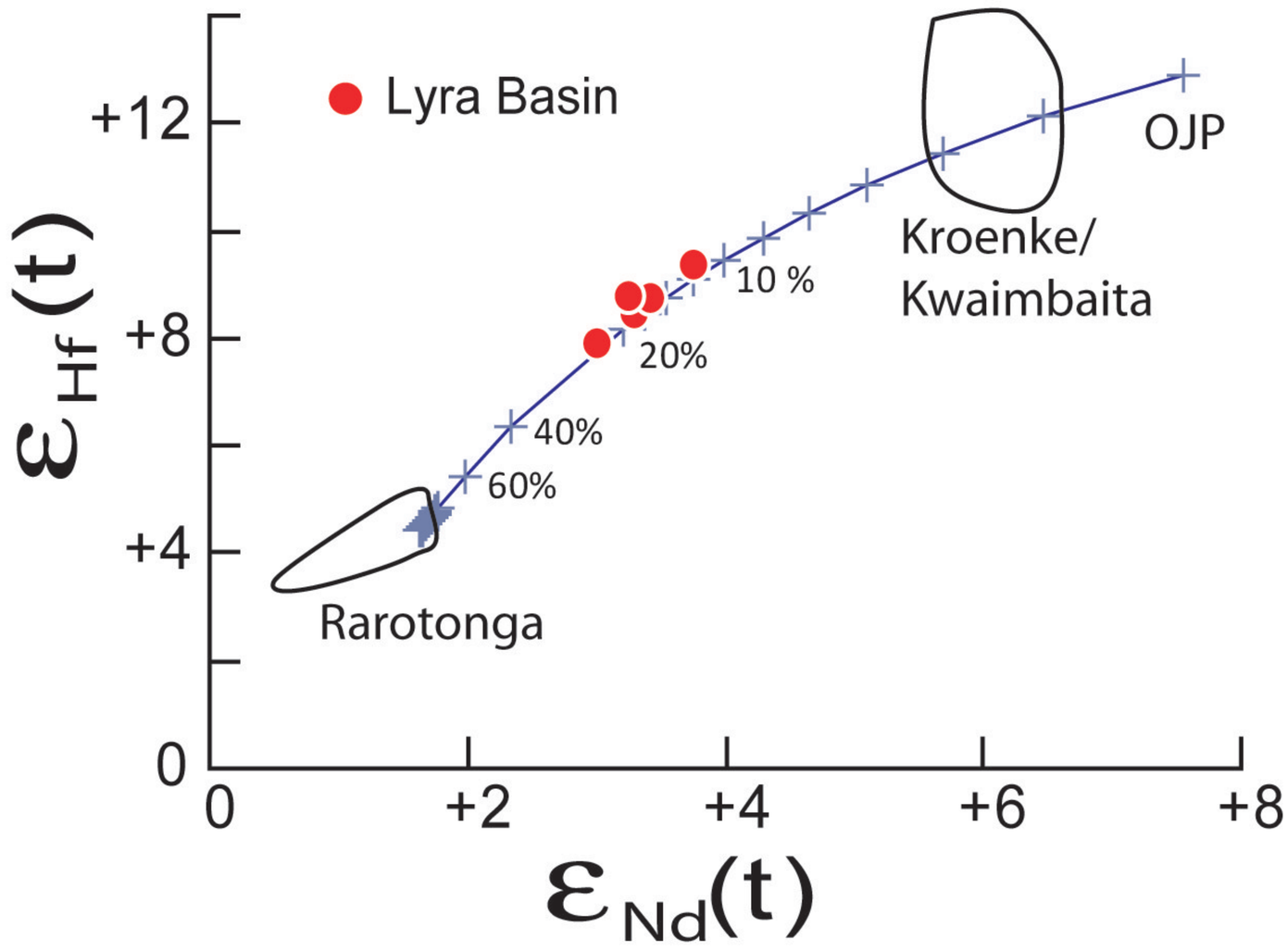

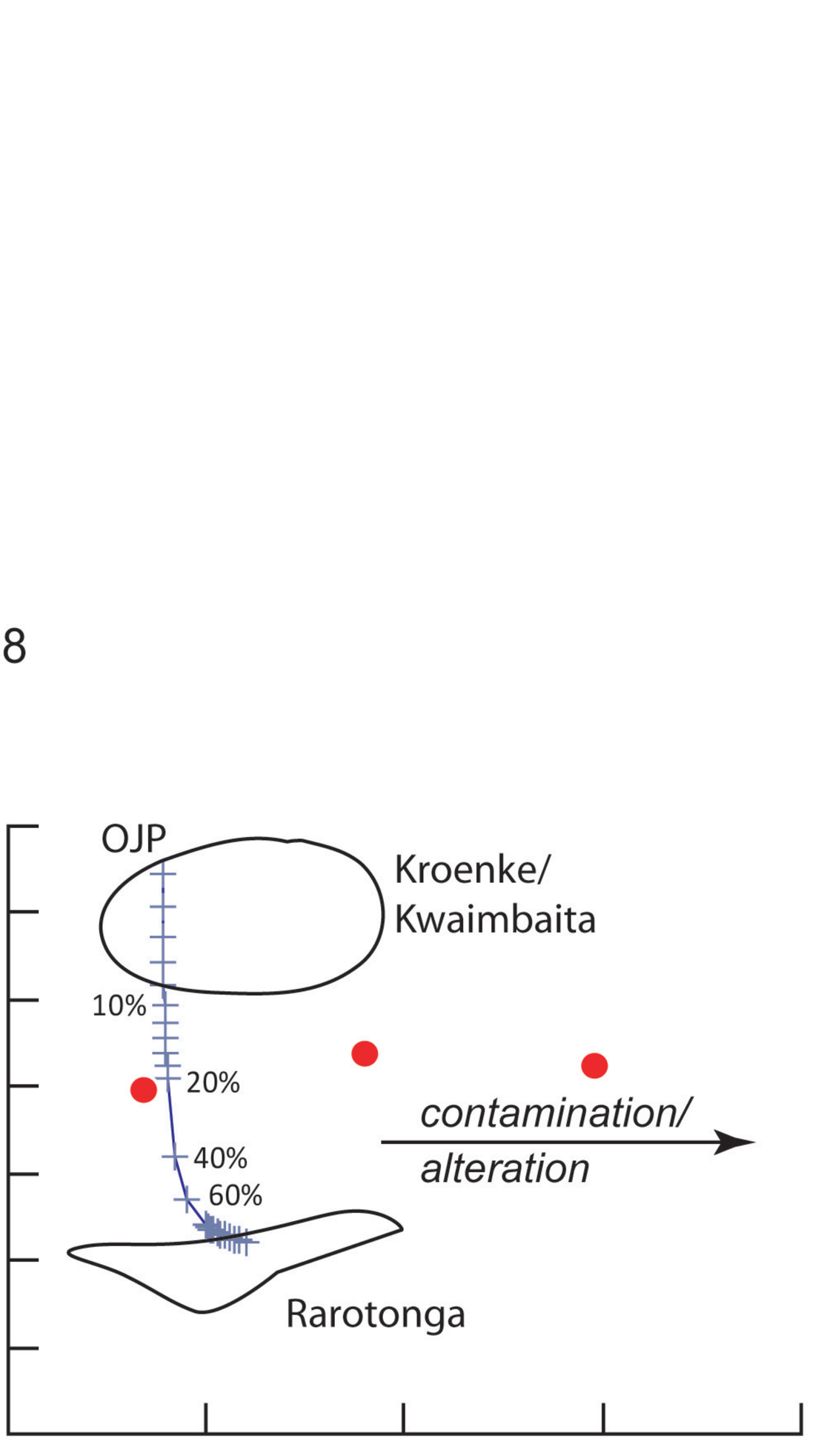

Figure 8, Tejada et al. 2014

TABLE 1. Pb-Nd-Sr ISOTOPE DATA

Sample No.	$^{87}Sr/^{86}Sr$ *2 SE*	$(^{87}Sr/^{86}Sr)t$	$^{143}Nd/^{144}Nd$ *2 SE*	$(^{143}Nd/^{144}Nd)t$	$\varepsilon_{Nd}(t)$	$^{206}Pb/^{204}Pb$ *2 SE*	$^{207}Pb/^{204}Pb$ *2 SE*	$^{208}Pb/^{204}Pb$ *2 SE*	$(^{206}Pb/^{204}Pb)t$	$(^{207}Pb/^{204}Pb)t$	$(^{208}Pb/^{204}Pb)t$
D1-06	0.705181	0.705105	0.512771	0.51271	3.0	18.727	15.585	38.741	18.570	15.577	38.542
	0.000007		*0.000010*			*0.002*	*0.002*	*0.004*			
D1-43	0.705046	0.704966	0.512770	0.51271	3.1	18.818	15.589	38.841	18.544	15.576	38.680
	0.000007		*0.000014*			*0.002*	*0.001*	*0.004*			
D2-07	0.704607	0.704513	0.512810	0.51275	3.8	18.572	15.560	38.605	18.534	15.558	38.467
	0.000006		*0.000012*			*0.001*	*0.001*	*0.003*			
D2-16	0.704705	0.704637	0.512789	0.51273	3.5	18.860	15.585	38.843	18.649	15.575	38.626
	0.000007		*0.000012*			*0.002*	*0.001*	*0.004*			
D2-18	0.704989	0.704936	0.512788	0.51272	3.3	18.707	15.577	38.701	18.488	15.567	38.486
	0.000008		*0.000012*			*0.001*	*0.001*	*0.003*			
D2-20	0.704985	0.704776	0.512786	0.51272	3.3	18.830	15.578	38.821	18.722	15.573	38.627
	0.000008		*0.000010*			*0.001*	*0.001*	*0.003*			
D1-06 CPX	0.705135	0.705100	0.512770	0.51270	2.8						
	0.000007		*0.000010*								
D2-18 CPX	0.704942	0.704863	0.512796	0.51272	3.3						
	0.000007		*0.000009*								

Notes: Uncertainties are reported as 2 standard errors, 2SE. Present-day Sr and Nd isotope ratios are relative to $^{87}Sr/^{86}Sr = 0.71026$ for SRM 987 and $^{143}Nd/^{144}Nd = 0.512101$ for JNd-1. Isotope compositions are age-corrected to 65 Ma. Age-corrected values are also bias-corrected relative to $^{87}Sr/^{86}Sr = 0.71024$ for SRM 987 and $^{143}Nd/^{144}Nd = 0.511850$ for La Jolla Nd standard in order to directly compare them with published data for OJP and younger alkalic rocks in Malaita and Santa Isabel (Mahoney et al., 1993; Tejada et al., 1996; 2002; 2004). Bias-correction for Nd isotope composition used the average of measured values for JNd-1, which is equivalent to 1.000503 times that of La Jolla Nd standard (Tanaka et al., 2000; Miyazaki et al., 2012). Parent-daughter concentrations used for age-correction of isotope ratios are reported in Table 3. Isotopic fractionation corrections are $^{86}Sr/^{88}Sr = 0.1194$ and $^{146}Nd/^{144}Nd = 0.7219$. Present-day $\varepsilon_{Nd}(t) = 0$ corresponds to $^{143}Nd/^{144}Nd = 0.512638$ for $^{147}Sm/^{144}Nd = 0.1967$; $\varepsilon_{Nd}(t) = 0$ at 65 Ma corresponds to $^{143}Nd/^{144}Nd = 0.512554$. Present-day Pb isotopic values are corrected for fractionation using double spike ^{207}Pb-^{204}Pb values of $^{206}Pb/^{204}Pb = 0.10203$, $^{207}Pb/^{204}Pb = 3.8717$, and $^{208}Pb/^{204}Pb = 0.18865$.

TABLE 2. Re-Os AND Lu-Hf ISOTOPE AND ABUNDANCE DATA

Sample number	Re (ppt)	*2SE*	Os (ppt)	*2SE*	$^{187}Os/^{188}Os$	*2SE*	$^{187}Re/^{188}Os$	*2SE*	$(^{187}Os/^{188}Os)_t$	Lu (ppm)	Hf (ppm)	$^{176}Hf/^{177}Hf$	*2SE*	$(^{176}Hf/^{177}Hf)t$	$\varepsilon_{Hf}(t)$
D1-06	205	0.2	515	2	0.1290	0.0002	1.9	<0.1	0.1269	0.081	2.92	0.282958	0.000009	0.28295	7.9
	128	0.2	741	2	0.1272	0.0002	0.8	<0.1	0.1263						
D1-37	89	0.1	90.9	0.3	0.1693	0.0015	4.8	<0.1	0.1641	0.167	5.50	0.282979	0.000009	0.28297	8.6
D2-02	58	0.1	31.0	<0.1	0.1936	0.0008	9.0	<0.1	0.1838	0.145	4.74	0.282960	0.000009	0.28295	7.9
D2-04	236	0.3	57.7	0.1	0.1852	0.0005	19.8	<0.1	0.1638	0.112	4.35	0.282970	0.000009	0.28297	8.3
D2-06										0.177	6.33	0.282976	0.000009	0.28297	8.5
D2-07										0.167	7.77	0.282998	0.000009	0.28299	9.3
D2-16										0.209	7.23	0.282983	0.000009	0.28298	8.7
D2-18	326	0.4	57.2	<0.1	0.1795	0.0004	27.6	<0.1	0.1496	0.124	4.83	0.282973	0.000009	0.28297	8.4
										0.105	4.02	0.282958	0.000009	0.28295	7.9
D2-20	202	0.2	81.6	0.1	0.1511	0.0003	12.0	<0.1	0.1381	0.122	3.76	0.282983	0.000009	0.28298	8.7
D2-23										0.172	6.33	0.282983	0.000008	0.28298	8.7
										0.095	3.26	0.282985	0.000009	0.28298	8.8
JB-1b										0.302	3.47	0.282973	0.000010		

Notes: Uncertainties are reported as two standard errors of the mean, 2SE. Data for $^{176}Hf/^{177}Hf$ are reported relative to 0.282160 measured for JMC475. Normalizing values for isotopic fractionation corrections are $^{179}Hf/^{177}Hf = 0.7325$. The $\varepsilon_{Hf}(t)$ values are calculated relative to bulk-earth value of $^{176}Hf/^{177}Hf = 0.282730$ corresponding to $\varepsilon_{Hf}(0) = 0$ at 65 Ma, estimated using $^{176}Hf/^{177}Hf = 0.282772$ corresponding to $\varepsilon_{Hf}(0) = 0$ today and $^{176}Lu/^{177}Hf = 0.0332$. Data for $^{187}Os/^{188}Os$ are normalized using $^{192}Os/^{188}Os = 3.08271$ and corrected using $^{18}O/^{16}O$ and $^{17}O/^{16}O$ of 0.002045 and 0.00371, respectively.

TABLE 3. PARENT-DAUGHTER ABUNDANCE DATA

Sample number		Rb (ppm)	Sr (ppm)	Sm (ppm)	Nd (ppm)	Th (ppm)	U (ppm)	Pb (ppm)
D1-06		3.0	148	3.80	14.34	1.32	0.344	1.39
	1SD	0.0	1	0.04	0.10	0.01	0.003	0.01
	RSD(%)	1.2	0.7	0.9	0.7	0.7	1.0	0.7
D1-43		17.4	801	6.31	24.7	1.67	0.936	2.18
	1SD	0.1	7	0.06	0.1	0.02	0.015	0.03
	RSD(%)	0.7	0.9	0.9	0.5	1.2	1.6	1.3
D2-07		23.9	891	5.47	20.9	1.38	0.128	2.10
	1SD	0.1	5	0.05	0.2	0.01	0.002	0.03
	RSD(%)	0.3	0.6	1.0	1.0	0.5	1.8	1.3
D2-16		13.5	780	5.71	22.9	3.03	0.971	2.94
	1SD	0.1	5	0.05	0.2	0.01	0.004	0.02
	RSD(%)	0.7	0.6	0.8	0.7	0.3	0.4	0.8
D2-18		4.91	419	5.17	19.0	1.34	0.450	1.31
	1SD	0.03	2	0.06	0.1	0.01	0.004	0.01
	RSD(%)	0.7	0.5	1.1	0.6	0.9	1.0	1.0
D2-20		38.5	553	5.16	18.8	1.19	0.218	1.29
	1SD	0.2	3	0.02	0.1	0.02	0.003	0.01
	RSD(%)	0.6	0.5	0.4	0.5	1.4	1.4	1.1
BHVO-2, ave.	(n = 6)	9.02	391	6.06	24.3	1.21	0.420	1.58
	1SD	0.36	13	0.08	0.2	0.02	0.017	0.28
	RSD(%)	3.9	3.2	1.3	0.8	1.8	4.1	18.0
Published *		9.11	396	6.07	24.5	1.22	0.403	1.6
JB-2, ave.	(n = 3)	6.33	173	2.24	6.25	0.252	0.148	5.01
	1SD	0.31	1	0.04	0.09	0.002	0.010	0.07
	RSD(%)	4.9	0.7	1.7	1.5	0.8	6.8	1.4
Published †		7.37	178	2.31	6.63	0.35	0.18	5.36

Notes: Concentrations were measured on splits of the same solutions measured for Sr and Nd isotopes and from the same leached powders used for Pb isotope analysis.

* and † refers to data sources for published values for BHVO-2 and JB-2, respectively:
*Geo-Reference Materials (GRM)
†Geological Survey of Japan (GSJ)

TABLE 4. MODELING PARAMETERS FOR RAROTONGA MELT-OJP SOURCE MIXING MODEL

Rarotonga melt/source composition recent (Hanyu et al., 2011)				Rarotonga melt/source at 95 Ma Magellan Smt., (Konter et al., 2008)		Values used Rarotonga melt at 65 Ma	
	low	high		low	high		
Hf	4	6				4	ppm
Os	0.032	0.188	ppb			0.21	ppb
Pb	0.16	0.27				0.20	ppm
Nd	17	22				22	ppm
$^{176}Hf/^{177}Hf$	0.28287	0.28291		0.28274	0.28283	0.28282	
$^{143}Nd/^{144}Nd$	0.51265	0.51275		0.51252	0.51274	0.51257	
$^{187}Os/^{188}Os$	0.124	0.139				0.13	
$^{206}Pb/^{204}Pb$	18.246	18.975		18.121	19.094	18.85	

OJP source at120 Ma			Parent-daughter ratios		OJP source at 65 Ma		Values used OJP source at 65 Ma	
Malaitan xenoliths (Ishikawa et al., 2007; 2011)			Malaitan xenoliths (Ishikawa et al., 2007; 2011)					
Hf	0.338	0.828					0.8	ppm
Os	0.728	4.94	ppb				0.8	ppb
Pb	0.021	0.028					0.03	ppm
Nd	2.06	2.94					2	ppm
Kroenke basalts (Tejada et al., 2004; 2013)					low	high		
$^{176}Hf/^{177}Hf$	0.28301	0.28307			0.28304	0.28318	0.28304	
$^{176}Lu/^{177}Hf$			0.0277	0.1000				
$^{143}Nd/^{144}Nd$	0.51280	0.51281			0.51287	0.51290	0.51287	
$^{147}Sm/^{144}Nd$			0.2126	0.2610				
$^{187}Os/^{188}Os$	0.1249	0.1322	0.1244	0.1270	0.1249	0.1330	0.1278	
$^{187}Re/^{188}Os$			0.05	0.83				
$^{206}Pb/^{204}Pb$	18.317	18.398			18.378	18.500	18.378	
$^{238}U/^{204}Pb$			7.07	11.93				

Notes: Magellan seamount data are interpreted as the ~95 Ma expression of Rarotongan hotspot based on backtracked locations (Konter et al., 2008). OJP lithospheric mantle source concentrations and parent-daughter ratios are assumed to be represented by garnet lherzolite xenoliths while the isotopic compositions are assumed to be expressed in Kroenke-type basalts